Advances in Water Resources 109 (2017) 236–252

Contents lists available at ScienceDirect

Advances in Water Resources

journal homepage: www.elsevier.com/locate/advwatres

Four decades of microwave satellite soil moisture observations: Part 2. Product validation and inter-satellite comparisons

L. Karthikeyan[a,b,*], Ming Pan[a], Niko Wanders[a,c], D. Nagesh Kumar[b], Eric F. Wood[a]

[a] Department of Civil and Environmental Engineering, Princeton University, NJ, USA
[b] Department of Civil Engineering, Indian Institute of Science, Bangalore, India
[c] Department of Physical Geography, Utrecht University, Utrecht, The Netherlands

ARTICLE INFO

Article history:
Received 27 February 2017
Revised 10 September 2017
Accepted 11 September 2017
Available online 15 September 2017

Keywords:
Soil moisture
Validation
ISMN
VIC
Passive microwave
Active microwave

ABSTRACT

Soil moisture is widely recognized as an important land surface variable that provides a deeper knowledge of land-atmosphere interactions and climate change. Space-borne passive and active microwave sensors have become valuable and essential sources of soil moisture observations at global scales. Over the past four decades, several active and passive microwave sensors have been deployed, along with the recent launch of two fully dedicated missions (SMOS and SMAP). Signifying the four decades of microwave remote sensing of soil moisture, this Part 2 of the two-part review series aims to present an overview of how our knowledge in this field has improved in terms of the design of sensors and their accuracy for retrieving soil moisture. The first part discusses the developments made in active and passive microwave soil moisture retrieval algorithms. We assess the evolution of the products of various sensors over the last four decades, in terms of *daily coverage*, *temporal performance*, and *spatial performance*, by comparing the products of eight passive sensors (SMMR, SSM/I, TMI, AMSR-E, WindSAT, AMSR2, SMOS and SMAP), two active sensors (ERS-Scatterometer, MetOp-ASCAT), and one active/passive merged soil moisture product (ESA-CCI combined product) with the International Soil Moisture Network (ISMN) in-situ stations and the Variable Infiltration Capacity (VIC) land surface model simulations over the Contiguous United States (CONUS). In the process, the regional impacts of vegetation conditions on the spatial and temporal performance of soil moisture products are investigated. We also carried out inter-satellite comparisons to study the roles of sensor design and algorithms on the retrieval accuracy. We find that substantial improvements have been made over recent years in this field in terms of daily coverage, retrieval accuracy, and temporal dynamics. We conclude that the microwave soil moisture products have significantly evolved in the last four decades and will continue to make key contributions to the progress of hydro-meteorological and climate sciences.

1. Introduction

Soil moisture (SM) is a key state variable modulating energy and water exchanges at the land and atmosphere interface. Better assessment of soil moisture dynamics improves our knowledge and monitoring capabilities of important land surface processes. Soil moisture determines the amount of water available for the evapotranspiration from land and thus plays a considerable role in moisture circulation in the atmosphere (Seneviratne et al., 2010). It impacts various climate process drivers such as precipitation (Guillod et al., 2015; Koster et al., 2004) and air temperature (Miralles et al., 2014), and controls the partitioning of precipitation into runoff and infiltration thereby affecting streamflow and ground water recharge in the hydrological cycle (Botter et al., 2007; Orth and Seneviratne 2013; Salvucci 2001). Due to its persistent memory, soil moisture helps improve the modeling of heatwaves (Miralles et al., 2014), droughts (Luo and Wood 2007), floods (Massari et al., 2014; Parinussa et al., 2016), thunderstorms (McColl et al., 2017), and crop yield (Rosenzweig et al., 2002). It plays a crucial role in managing the plant growth by which the carbon cycle is regulated (D' odorico et al. 2003). Soil moisture is deemed to be an essential variable to improve the accuracy of long term as well as seasonal scale numerical weather forecasts (de Rosnay et al. 2014; Dirmeyer and Halder 2016; Drusch 2007). Soil moisture is also one of the best indicators for agricultural and ecological droughts (Mo 2008; Sheffield and Wood 2007). In the era of increased awareness towards climate change, information about soil moisture is observed in several studies to influence the simula-

* Corresponding author at: Department of Civil Engineering, Indian Institute of Science, Bangalore, India.
E-mail address: karthik120120@gmail.com (L. Karthikeyan).

http://dx.doi.org/10.1016/j.advwatres.2017.09.010
0309-1708/

tions of future projections of climate variables such as temperature (Vogel et al., 2017), precipitation (May et al., 2015) and evapotranspiration (Seneviratne et al., 2013).

Observing soil moisture at large spatial scales has been a very difficult task for ground sensors given the highly heterogeneous nature of soil moisture in both time and space (due to variability in climate/weather, snow, topography, vegetation, land use, water table depth and soil type). This variability may not allow us to generalize regional scale findings to global scales while geographical, financial and political constraints limit the development of dense station networks in many parts of the world (Crow et al., 2005; Karthikeyan and Kumar 2016; Pan and Wood 2009; Prigent et al., 2005). With the advent of remote sensing, the retrieval of surface soil moisture from microwave sensors has drawn the attention of hydro-meteorologists, climate and agricultural scientists over the past four decades. Its global availability and increased temporal and spatial resolutions have resulted in increasing use of these products for research and operational purposes. Microwave sensors are categorized into *passive sensors* and *active sensors*. The passive sensors detect the natural microwave radiations emitted from the ground in the form of brightness temperature measurements (T_B). The active sensors send radiation pulses towards the Earth surface and detect the reflected and scattered signals as backscatter coefficients (σ_o).

The passive and active microwave satellite sensors have been providing useful global scale surface soil moisture retrievals since 1978 (Colliander et al., 2017; Entekhabi et al., 2010a; Jackson 1997; Jackson et al., 2002; Kerr et al., 2016; Kerr et al., 2012; Kerr et al., 2001; Liu et al., 2012; McCabe et al., 2005; Njoku et al., 2003; Njoku and Li 1999; Njoku et al., 1998; O'Neill et al., 2016b; Owe et al., 2008; Pan et al., 2014; Parinussa et al., 2015; Piepmeier et al., 2017; Wagner et al., 1999; Wagner et al., 2003; Wanders et al., 2012). The series of passive microwave sensors contributing to global scale soil moisture retrievals include the Scanning Multichannel Microwave Radiometer (SMMR), the Special Sensor Microwave - Imager (SSM/I), the microwave imager of Tropical Rainfall Measuring Mission (TMI), the WindSAT mission, the Advanced Microwave Scanning Radiometer – Earth Observing System (AMSR-E), the Advanced Microwave Scanning Radiometer 2 (AMSR2) mission, the Soil Moisture Ocean Salinity (SMOS) mission, and the Soil Moisture Active Passive (SMAP) mission. In case of active sensors, the Scatterometers of the European Remote Sensing (ERS-1/2) satellites and the Advanced Scatterometer (ASCAT) of the Meteorological Operational satellite program (MetOp-A/B) (2007–2014) provide the global scale soil moisture retrievals. With this legacy of soil moisture sensors, efforts have been directed towards merging the passive and the active microwave soil moisture products under the European Space Agency (ESA) Climate Change Initiative (CCI) program in an attempt to create a long term global scale soil moisture record (Liu et al., 2012; Liu et al., 2011).

Given the indirect nature of soil moisture remote sensing, validation is an important and also challenging aspect of satellite soil moisture retrievals. The most direct form of validation is to compare the retrievals with in-situ station observations subject to availability of data (Al Bitar et al. 2012; Chan et al., 2016; Dorigo et al., 2015; Jackson et al., 2010; Wu et al., 2016). Currently, the International Soil Moisture Network (ISMN) provides observations of soil moisture and other ancillary variables on a public platform corresponding to 2226 stations (as of 16 February 2017; Fig. 1 presents the spread of stations over the Contiguous United States) (Dorigo et al., 2011). Furthermore, field campaigns such as the campaign for validating the operation of SMOS (coSMOS) (Delwart et al., 2008) and the SMAP Validation Experiment 2016 (SMAPVEX16) (Chan et al., 2016; Colliander et al., 2015) have been implemented that support calibration and validation of SMOS and SMAP missions respectively. Since ground observations are not available globally and are typically representative of different spatial scales than satellite based retrievals, alternate validation techniques such as triple collocation (Gruber et al., 2016; Pan et al., 2016; Pan et al., 2015; Scipal et al., 2008), R_{value} (Crow 2007; Crow et al., 2010; Crow and Zhan 2007) and mutual information based approaches (Karthikeyan and Kumar 2016; Tuttle and Salvucci 2014) have been developed. Furthermore, the soil moisture output from land surface models (LSMs) – which simulate the soil moisture (Koster et al., 2009) state along with other states and fluxes using forcing and ancillary datasets – can be used to assess the accuracy of the satellite soil moisture retrievals (Fang et al., 2016; Pan et al., 2016). In fact, many efforts have been made to assimilate soil moisture retrievals into LSMs to improve the estimates of soil moisture (De Lannoy and Reichle 2016; Pan and Wood 2010; Reichle et al., 2008; Reichle et al., 2016; Yan and Moradkhani 2016), streamflow (Alvarez-Garreton et al., 2016; Wanders et al., 2014a; Wanders et al., 2014b) and precipitation (Wanders et al., 2015; Zhan et al., 2015).

In Part 1 (Karthikeyan et al., 2017) of this two-part-review series, we looked at the development of passive and active microwave soil moisture retrieval algorithms over the last four decades. The study area is set to the Contiguous United States (CONUS) for all analyses. Here in Part 2, we provide a systematic overview of the evolution of microwave satellite sensors and their retrieval performance over the past four decades. The paper is arranged in the following manner. Section 2 gives a summary of the instrument features of passive and active sensors along with the details regarding reference data used for comparison purposes. Section 3 discusses how improvements have been made in terms of *daily coverage*, *spatial performance* and *temporal performance* of soil moisture products with an emphasis on regional validation and inter-sensor comparisons.

2. Data and methods

The present validation paper focuses on evaluating the microwave soil moisture products of eight passive, two active, and one combined active/passive sensors over the Contiguous United States (CONUS). SMMR, SSM/I, TMI, WindSAT, AMSR-E, AMSR2, SMOS, and SMAP are the passive sensors. ERS Wind Scatterometer, hereafter referred to as "ERS" and MetOp ASCAT, hereafter referred to as "ASCAT", are the active sensors. The combined active/passive soil moisture product developed by the European Space Agency (ESA) under their 'Climate Change Initiative (CCI)' is also validated in this work. The following sub-sections provide a brief overview of the passive and active sensors' configuration and their evolution over time. The soil moisture products corresponding to these sensors are evaluated with respect to ISMN station data and VIC land surface model simulations. Hence, the subsequent sub-sections provide a description of these datasets followed by a description of the methodology involved in the analyses.

Table 1 summarizes configuration of passive and active microwave sensors described in the sections below.

2.1. Passive microwave sensors

2.1.1. Scanning multichannel microwave radiometer (SMMR)

The Scanning Multichannel Microwave Radiometer (SMMR), launched onboard the National Aeronautics and Space Administration's (NASA) Nimbus-7 satellite in 1978, was the first passive microwave satellite sensor that had the capability of retrieving surface soil moisture. Primarily, it was launched for obtaining Sea Surface Temperature (SST), surface wind speed, water vapor, and cloud

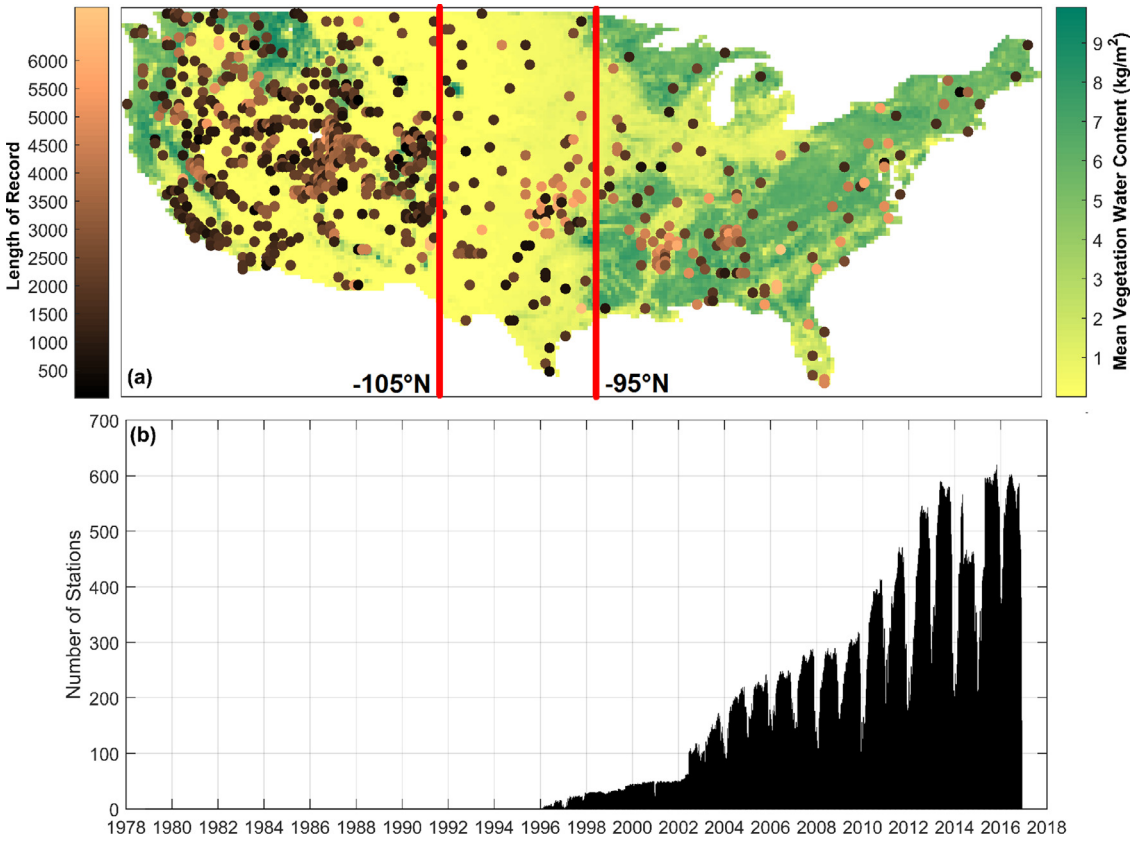

Fig. 1. (a) Spatial spread of ISMN stations with their length of record in days plotted over mean vegetation water content (kg/m^2) map; (b) Time evolution of number of ISMN stations over the CONUS. Notice the decrease in wintertime due to snow and frozen ground. The two red lines in the spatial map are −105°N and −95°N longitudes which divide the CONUS into three (*western, central* and *eastern*) regions to evaluate the regional performance of soil moisture products in Section 3.

Table 1
Summary of passive and active microwave sensors.

Instrument	Satellite	Duration	Frequency (GHz)	Footprint size (km)	Incidence angle at earth surface (°)	Temporal resolution (Days)	Coverage
SMMR	Nimbus 7	Oct 1978 - Aug 1987	6.6 10.7	148 × 95 91 × 59	50.2	2	Global
SSM/I	DMSP	Aug 1987 - Dec 2007	19.3	70 × 45	53.1	1	Global
TMI	TRMM	Dec 1997 - Apr 2015	10.7	59 × 36	35	1	N40° to S40°
AMSR-E	Aqua	Jun 2002 - Sep 2011	6.9 10.7	76 × 44 49 ×28	55	1	Global
WindSAT	Coriolis	Feb 2003 - Jul 2012	6.8 10.7	60 × 40 38 × 25	53.5 49.9	1	Global
AMSR2	GCOM-W	Jul 2012 - Present	6.9 10.7	62 × 35 42 × 24	55	1	Global
MIRAS	SMOS	Jan 2010 - Present	1.4	35–50	0–55	1–3	Global
SMAP	SMAP	Mar 2015 - Present	1.4	47 × 39	40	1–3	85.044°N - 85.044°S
ERS	ERS-1/2	July 1991–Sep 2011	5.3	50 × 50	16–50	2–7	Global
ASCAT	MetOp-A/B	Jan 2007–Present	5.225	25 × 25	25–65	1–2	Global
ESA-CCI-COMBI	Various	Oct 1978-Dec 2014	Various	25 × 25	Various	1	Global

liquid water content information. The five dual polarized frequencies from 6.6 to 37 GHz provided brightness temperatures every other day (due to power limitations) (Gloersen and Hardis 1978). SMMR global repeat coverage was up to six days. Since there is no publicly available soil moisture product pertaining to SMMR sensor, we obtained corresponding data from ESA-CCI passive soil moisture (Liu et al., 2012; Liu et al., 2011) product, which retrieved soil moisture using the X-band brightness temperature data (having a penetration depth of ~0.3–1 cm) using the LPRM algorithm. Note that the penetration depth of passive microwave signals is on the order of one tenth of the wavelength but can become deeper for dryer soil and due to surface roughness (Ulaby et al. 1986).

2.1.2. Special sensor microwave imager (SSM/I)

The Special Sensor Microwave Imager (SSM/I) of the Defense Meteorological Satellite Program (DMSP)-F08 satellite continued the legacy of SMMR since its launch in 1987. It had onboard seven channels with frequencies ranging from 19.3 GHz to 85.5 GHz. Its purpose was to obtain ocean wind speed, atmospheric water vapor, cloud liquid water, and rain rate information. With an improved swath width (1400 km) and reduced power consumption, SSM/I achieved global coverage almost daily (Noll et al., 1994). Due to advancements in antenna characteristics and data preprocessing, the performance of SSM/I was improved over its predecessors. SSM/I continued to provide data until June 2002. Even in this case, we

could not obtain an official soil moisture product. Hence, the soil moisture retrievals made exclusively with the SSM/I sensor data (using 19.3 GHz horizontal and vertical frequency channels; having a penetration depth of ~0.15–0.5 cm) under the ESA-CCI passive soil moisture product (using LPRM retrieval algorithm) (Liu et al., 2012; Liu et al., 2011) are used in our analysis.

2.1.3. Tropical rainfall measuring mission (TRMM) – microwave imager (TMI)

The Tropical Rainfall Measuring Mission (TRMM)'s Microwave Imager (TMI) was one of the three sensors onboard the TRMM satellite launched in 1997 jointly by NASA and National Space Development Agency (NASDA) of Japan. The satellite was launched primarily for measuring rainfall and energy exchange in the tropical and subtropical regions (Bindlish et al., 2003). Launched as a successor to SSM/I, the TMI had dual polarized frequencies of 10.65, 19.4, 21.3, 37, and 85.5 GHz. The TMI made two daily passes (ascending and descending) at a location with a near-equatorial orbit. The TMI had a higher spatial resolution than that of SSM/I due to its larger antenna and lower orbital altitude. In 2001, an orbital maneuver boost of TRMM (increase in orbital altitude) increased the instrument lifetime and swath width which consequentially reduced the spatial resolution (from 50 km to 51 km for X-band) of the sensor. The soil moisture retrievals used in this analysis are obtained from the LPRM retrieval algorithm (using X-band brightness temperature data) created by Vrije Universiteit Amsterdam (VUA) and NASA Goddard Space Flight Center (GSFC) (De Jeu 2012a, b; Owe et al., 2008).

2.1.4. Advanced microwave scanning radiometer for the earth observing system (ASMR-E)

The Advanced Microwave Scanning Radiometer for the Earth Observing System (ASMR-E) onboard NASA's Aqua satellite (dedicated for remote sensing of climate and hydrology) was developed jointly by Japan's Aerospace Exploration Agency (JAXA) and NASA. It was launched in 2002 (Kawanishi et al., 2003). AMSR-E provided support to EOS mission objectives of Aqua satellite by primarily measuring precipitation rate, cloud water, water vapor, sea surface winds, sea surface temperature, sea ice concentration, snow water equivalent, and soil moisture variables. The sensor had six frequencies (6.92, 10.65, 18.7, 23.8, 36.5, and 89.0 GHz) in horizontal and vertical polarizations. The polar orbiting AMRE-E achieved global coverage within two days separately for ascending and descending passes (except for a few polar regions). The spatial resolution of AMSR-E improved significantly over SMMR (from 150 km to 50 km for C-band radiometer) while also containing all channels of the previous sensors (SMMR, SSM/I and TMI). The sensor stopped operating in 2011 due to an antenna failure. Given its long data record (~10 years) across 12 channels, AMSR-E created new opportunities towards the development of the soil moisture retrieval algorithms. In this regard, we considered two soil moisture products (using X-band radiometer, having a penetration depth of ~0.3–1 cm), which are produced with two different retrieval algorithms LSMEM (Pan et al., 2014) and LPRM (De Jeu 2011a, b; Owe et al., 2008).

2.1.5. WindSAT

The WindSAT sensor was the first fully polarimetric (consisting of horizontal, vertical, linear and circular polarizations) microwave radiometer, launched in 2003 on the Coriolis satellite developed by the Naval Research Laboratory Remote Sensing Division, the Naval Center for Space Technology for the U.S. Navy and the National Polar-orbiting Operational Environmental Satellite System (NPOESS) Integrated Program Office (IPO) (Gaiser et al., 2004). The polar orbiting WindSAT had 5 frequencies (6.8, 10.7, 18.7, 23.8 and 37 GHz) all of them fully polarimetric except 6.8 and 23.8 GHz channels, with a revisit time of one day. WindSAT was intended for weather forecasts and warnings, nowcasting, climatology, and oceanography studies. It provides data related to sea surface wind speed and sea surface wind direction, column integrated cloud liquid water, column integrated precipitable water, and sea surface temperature (Gaiser et al., 2004). The WindSAT was a successor to ASMR-E with spatial resolution (38 km for X-band radiometer) and polarimetric capabilities. Here, we use the soil moisture product developed using X-band radiometer observations (having a penetration depth of ~0.3–1 cm) and the LPRM retrieval algorithm for the analysis given in Section 3 (De Jeu 2012a, b; Owe et al., 2008).

2.1.6. Advanced microwave scanning radiometer 2 (AMSR2)

The Advanced Microwave Scanning Radiometer 2 (AMSR2) developed jointly by NASA and JAXA was launched in 2012 onboard the JAXA's Global Change Observation Mission - Water "SHIZUKU" (GCOM-W), as a continuation mission to AMSR-E. It has all the frequency channels and similar sensor configuration as that of AMSR-E with an additional C-band (7.3 GHz) dual polarization frequency to improve the mitigation of the Radio Frequency Interference (RFI). It was launched for the retrieval of integrated water vapor, integrated cloud liquid content, precipitation, sea surface temperature, sea surface wind speed, sea ice concentration, snow depth and soil moisture. The satellite has a revisit time of one day. The instrument has a higher spatial resolution due to the presence of a larger main antenna reflector. The AMSR2 is an operational sensor with the ability to obtain near-real time soil moisture retrievals. We used the official soil moisture product of GCOM-W *Version 2*, which uses the JAXA retrieval algorithm at X-band (having a penetration depth of ~0.3–1 cm) for the present analysis (Koike et al., 2004; Maeda and Taniguchi 2013).

2.1.7. Soil moisture ocean salinity (SMOS)

The Soil Moisture Ocean Salinity (SMOS) is the first dedicated satellite mission intended for global scale soil moisture and ocean salinity retrievals. Launched in 2009, the Microwave Imaging Radiometer with Aperture Synthesis (MIRAS) instrument, onboard the SMOS satellite was developed by Centre d'Etudes Spatiales de la Biosphère (CESBIO) with support from the European Space Agency (ESA), the Centre National d' Etudes Spatiales (CNES), and the Centro Para el Desarrollo Tecnologico Industrial (CDTI). This mission marked the first use of dual polarized L-band (1.4 GHz) 2-D passive interferometer radiometer. Measuring long wavelength microwave radiations requires a bigger antenna, which is achieved with a novel 'Y' shaped design embedded with 69 smaller antennas (called LICEFs), each measuring the Earth's surface emissions at L-band. SMOS is a sun-synchronous polar orbiting satellite and achieves global coverage every three days. The project target is to retrieve soil moisture with 0.04 m^3/m^3 accuracy. The usage of longer wavelength results in an ability to retrieve soil moisture from greater depth (~5 cm). Another unique feature of SMOS lies in its ability to measure brightness temperatures at multiple incidence angles in the range 0–50° With six years of successful operation, SMOS provides a processed (level 3) soil moisture product (through Centre Aval de Traitement des Données SMOS – CATDS, using the 'SMOS Soil Moisture Retrieval Algorithm' *Version 300* (Kerr et al., 2012)) at one week lag, which is used in our analysis.

2.1.8. Soil moisture active passive (SMAP)

The Soil Moisture Active Passive (SMAP) satellite mission is the most recent microwave sensor dedicated to obtaining surface soil moisture observations. It was launched in 2015 by NASA, with the objective of generating global fields of soil moisture and landscape freeze/thaw state (Entekhabi et al., 2014). The mission concept was to utilize the respective advantages offered by using both passive

and active sensors in retrieving soil moisture and to obtain accurate soil moisture observations with high spatial and temporal resolutions. In this regard, SMAP has two components: an active synthetic aperture radar (1.2 GHz with *VV, HH*, and *HV* polarizations) and a passive radiometer at L-band frequency (1.41 GHz with, V, H, the third and the fourth Stokes' parameters), and achieves global coverage every 2–3 days. Since the SMOS satellite has a dominant effect of RFI, the SMAP mission has incorporated stringent RFI filtering for both radiometer and radar sensors (Colliander et al., 2017). Unfortunately, after 11 weeks of operation, the radar instrument encountered a failure, although the radiometer continues its operations. The instrument is equipped with 6 m rotating conical scanning mesh reflector antenna revolving in a sun-synchronous near-polar orbit at an altitude of 685 km. The target accuracy of SMAP mission is 0.04 m^3/m^3. It has to be noted that this target accuracy corresponds to the unbiased Root Mean Square Error (ubRMSE), which is computed using data subject to a number of conditions, including – but not limited to – the vegetation water content threshold (of 5 kg/m^2). Other parameters are the presence of frozen soil, urban areas, active precipitation, etc. The SMAP soil moisture product in our analysis is the Level 3 *Version 4* dataset obtained as a composite of the Level 2 retrievals produced with the baseline *V*-polarization Single Channel Algorithm (V-SCA) (O' Neill et al. 2016a).

2.2. Active microwave sensors

2.2.1. Active microwave instrument – wind scatterometer (ERS)

The Active Microwave Instrument – Wind Scatterometer (ERS) was the first active sensor that is capable of retrieving soil moisture observations. Primarily intended for wind monitoring, the first ERS was launched onboard European Remote Sensing (ERS-1) satellite in 1991, which discontinued operation in 2000. The second instrument with the same configuration as its predecessor was launched onboard ERS-2 in 1995. The instrument was designed with fan-beam geometry with antennas oriented at 45°, 90°, and 135° with respect to satellite track. The ERS is a C-band (5.3 GHz) scatterometer (having a penetration depth of ~1–3 cm) with three vertically polarized antennas and a swath width of 500 km. The ERS had a revisit time of 2–7 days. The ERS signal was used to create the ESA-CCI active soil moisture product (which is used in the current work) by implementing the TU-Wien change detection algorithm within the Soil Water Retrieval Package (WARP). Due to an instrument fault, the sensor produced data discontinuously since 2001 until its end of the mission in 2010, hence, after the launch of the ASCAT sensor (onboard MetOp-A) in 2006, the usage of ERS has been discontinued (Crapolicchio and Lecomte 2004; Liu et al., 2012) (although soil moisture data are in principle available until the end of the mission) resulting in an ERS-based soil moisture product from 1991–2006.

2.2.2. Advanced scatterometer (ASCAT)

The Advanced Scatterometer (ASCAT) missions are active radar sensors which are successors to ERS. The first ASCAT was launched in 2006 onboard ESA's European Organization for the Exploitation of Meteorological Satellites (EUMETSAT) meteorological operational satellite (MetOp-A) (Bartalis et al., 2007). It started operating in 2007. Later, the second ASCAT instrument was deployed in 2012 onboard the MetOp-B satellite. The third ASCAT sensor is scheduled for launch in 2018. The primary objective of ASCAT is to obtain global ocean wind vectors, although it can also be used to monitor soil moisture, freeze/thaw states and sea ice (Figa-Saldaña et al., 2002). The ASCAT is a C-band (5.225 GHz) real aperture radar (having a penetration depth of ~1–3 cm) with three vertically polarized antennas. The ASCAT had an improved sensor configuration compared to its predecessors in terms of having dual swaths that improved the spatial coverage and improved the on-board calibration concept. Being a dedicated instrument (which results in no operational sharing time), the ASCAT had improved the revisit time to 1–2 days and attained the spatial resolution of 25 km. The instrument achieves global coverage in about 1.5 days. Apart from mission objectives, the ASCAT is also used for retrieving information about polar ice, soil moisture, and vegetation. The ASCAT soil moisture retrievals, even here, are obtained from the ESA-CCI active soil moisture product. In the case of multiple soil moisture retrievals in a day, the product averages these values (Liu et al., 2012).

2.3. ESA-CCI merged soil moisture

ESA under the Climate Change Initiative (CCI) has developed a quarter degree resolution global scale daily long term soil moisture record (Version 2.2) by systematically combining the retrievals from active and passive microwave soil moisture sensors. Passive microwave observations from SMMR, SSM/I, TMI, AMSR-E, and AMSR-2 have been combined with active microwave observations from ERS and ASCAT. The LPRM v5 and the change detection method TU Wien WARP v5.5 are utilized for producing soil moisture retrievals from passive and active microwave sensors respectively. The merging is carried out using a CDF based approach (Liu et al., 2012). The time period of the combined active and passive microwave sensors' product (referred as ESA-CCI-COMBI hereafter) is from 1978 to 2014 (Liu et al., 2012; Liu et al., 2011).

2.4. In-situ observations

The performance of active and passive soil moisture products is assessed by comparing them with station data procured from the International Soil Moisture Network (ISMN) Dorigo et al., 2011). ISMN is a publicly available global in-situ database intended for validation of satellite soil moisture observations as well as land surface model simulations. Data pertaining to 1058 stations over the CONUS were extracted from the ISMN. These stations are from a variety of networks; namely, ARM (29), COSMOS (2), FLUXNET-AMERIFLUX (2), iRON (6), PBO–H2O (138), SCAN (215), SNOTEL (425), SOILSCAPE (127), USCRN (110), and USDA-ARS (4). The numbers in parenthesis after each network indicate the total number of stations from the network that are in the ISMN. The soil moisture observations are corrected for quality using the flags provided by ISMN (Dorigo et al., 2013). The quality control resulted in discarding ~13% of the observations. Not shown here, applying the quality flags improved the results of comparison. Several of the stations report sub-daily scale measurements, in which case they are averaged to obtain a time series of daily average values. Additionally, only stations that have soil moisture observations for the top 5 cm soil layer are used since this is the sensitive region for satellite soil moisture retrievals. Fig. 1(a) presents the spatial distribution of stations, along with their record length (in days), overlaid on a mean vegetation water content map (derived from MODIS Leaf Area Index (LAI) product MOD15A2 (Myneni et al., 2002); the details of vegetation water content calculation procedure can be found in Wood et al. (2009)), and Fig. 1(b) shows a plot of the evolution of number of stations over the CONUS. It can be observed from Fig. 1(a) that stations with longer record lengths are mostly situated in the *central* CONUS with grassland/cropped land cover. Also, several new stations have been set-up in the *western* CONUS, however, very few stations exist in the *eastern* CONUS, which is due to the presence of dense forests. Fig. 1(b) shows that there is no available station data in the ISMN prior to 1996. Also, note the strong seasonality of available data that is related to snow cover and frozen ground. Further processing of the station observations is presented in Section 2.6.

2.5. VIC land surface model simulations (VIC-SM)

The Variable Infiltration Capacity (VIC) model (Liang et al., 1994; Liang et al., 1996) version 4.0.5 was used to simulate the surface hydrology from 1979 to present at 0.125° resolution and hourly time step over the CONUS area. VIC model calculates the exchanges of moisture and energy between the atmosphere and land surface, and between different soil layers. The infiltration parameterization is based on the concept of a statistically distributed soil water holding capacity for an upper soil moisture store, and the vertical movement of soil moisture among a 0.10 m surface layer, an upper and lower soil moisture stores. The upper and lower stores are calibrated (Troy et al., 2008). For the analysis here, VIC is forced with the surface meteorological fields from the National Land Data Assimilation System phase 2 (NLDAS-2) project (Xia et al., 2012), which combines both in-situ observations (rain gauges), rain radar, and numerical weather model reanalysis. VIC model has been widely used, calibrated and validated over different regions and the NLDAS-2 is also considered one of the most reliable sources of surface meteorological forcings. In the current work, the surface layer (0.10 m) soil moisture (VIC-SM) was used for the analysis.

2.6. Data processing

In order to carry out a comparative analysis between satellite products, station data, and land surface model simulations, it is important to bring these datasets to a consistent spatio-temporal framework. We used the Level 3 products developed under the respective soil moisture sensors (both active and passive). Except for SMOS and SMAP, the soil moisture products are available at quarter degree (0.25° × 0.25°) resolution on equal distance cylindrical projection grids. Thus, this projection and resolution are selected as the reference for our analysis. SMOS data is available in the Equal-Area Scalable Earth Grid – EASE (version 2) cylindrical projection grid system (Brodzik et al., 2012) at a 25 km spatial resolution (https://earth.esa.int/documents/10174/1854456/SMOS-Data-Products-Brochure). SMAP radiometer soil moisture product SM_L3_P is provided at a 36 km spatial resolution in the EASE (version 2) cylindrical projection grid system. These two products are re-gridded to the reference grid system (quarter degree) using inverse distance weighting average method. The average value of ascending and descending pass retrievals is considered as representative soil moisture value of that day at a particular location. The ISMN data are matched with the reference grid system. In the case of multiple stations within a grid, we used an unweighted arithmetic mean to represent the grid value. The 1058 stations resulted in 736 grid cells with station data over the CONUS.

There are systematic differences among the soil moisture data sets (8 from passive radiometer retrievals, 2 from active radar retrievals, 1 combined active/passive data, 1 VIC land surface model estimate and 1 up-scaled in-situ) due to (1) time of measurement, (2) scale mismatch among the products, (3) uncertainty and representativeness of the up-scaled station data, (4) uncertainty in the VIC-SM simulations due to process representation and parameter values, and (5) satellite measurement and retrieval algorithms that also include reporting radiometer products in volumetric units (m^3/m^3) and active products in degree of saturation (%). In order to minimize the impact of these differences and allow for a fair comparison of the product performance, we have applied cumulative density function (CDF) matching for all products using the up-scaled in-situ data as the reference. This ensures that the performance measures computed across the products are comparable. It has to be noted that the CDF matching is performed independently at each grid location. Although bias correcting the satellite products at locations with shorter record lengths might require additional treatment in terms of spatial sampling (Reichle and Koster 2004), such an analysis is beyond the scope of the current work.

We have evaluated the soil moisture products in three aspects: *coverage, temporal performance*, and *spatial performance*. Coverage for a particular product at daily scale is calculated as a fractional area over the CONUS with successful soil moisture retrievals (expressed in %) made in a day (t) (Eq. 1).

$$Coverage_t = \frac{(Area\ of\ succesful\ retrievals)_t}{Area_{CONUS}} \times 100 \tag{1}$$

In order to indicate the coverage achieved when all the products are combined i.e., to check the fractional area with successful retrievals from any of the products, a joint coverage time series was created. It has to be noted that the joint coverage doesn't include the AMSR2 product due to a low level of quality control and filtering in its retrievals. Root Mean Square Error ($RMSE$) and correlation (R) are used to compare the satellite soil moisture products (m_v^{sat}) with station data (m_v^{obs}) and with the VIC-SM (m_v^{VIC}). Temporal performance is assessed by computing $RMSE^{temporal}$ and $R^{temporal}$ at grids (N_i – length of record of i^{th} station) containing station data (see Eq. 2). Apart from these metrics, the temporal performance is further assessed using bias ($B^{temporal}$) (Eq. 3), scale error ($S^{temporal}$) (Eq. 4), anomaly $RMSE$ ($A-RMSE^{temporal}$), and anomaly R ($A-R^{temporal}$) (see Eq. 5) which are computed using the original soil moisture products (denoted by $\tilde{m}_v^{sat}$). The spatial performance of soil moisture products is evaluated by computing $RMSE^{spatial}$ and $R^{spatial}$ for each day (t) across all the grids where stations (ϕ – number of stations) are located (see Eq. 6). In the process of carrying out temporal and spatial validation, only locations and days with more than 20 observations are considered in order to remove the effect of undersampling. In order to understand the effect of vegetation conditions on the quality of retrievals, the performance of soil moisture products is evaluated at regional scale by splitting the CONUS into three regions, *the western* CONUS (the area to the left of −105°N longitude; containing stations at 510 grid cells), *the central* CONUS (the area between −105°N and −95°N longitudes; containing stations at 96 grid cells), and *the eastern* CONUS (the area to the right of −95°N longitude; containing stations at 130 grid cells). Corresponding to this analysis, the median values of temporal and spatial performance metrics, are presented as the summary statistics for the three regions and the CONUS. An $RMSE$ of 0.04 m^3/m^3 is considered as the target accuracy in our analysis. Finally, median values of temporal cross correlations (computed as the median value of temporal cross correlations obtained across all possible grid locations) between m_v^{sat}, m_v^{obs} and m_v^{VIC} are also computed over the CONUS to assess the amount of similarity offered by the products during their overlap period.

$$RMSE_i^{temporal} = \sqrt{\frac{\sum_{t=1}^{N_i}\left(\left[m_{v,t}^{sat}\right]_i - \left[m_{v,t}^{obs}\right]_i\right)^2}{N_i}}$$

$$R_i^{temporal} = \frac{\mathrm{cov}\left(m_v^{sat}, m_v^{obs}\right)}{\sigma_{m_v^{sat}}\sigma_{m_v^{obs}}}, \begin{cases}\mathrm{cov} - \text{covariance}\\ \sigma - \text{standard deviation}\end{cases} \tag{2}$$

$$B_i^{temporal} = \frac{\sum_{t=1}^{N_i}\left(\tilde{m}_{v,t}^{sat} - m_{v,t}^{obs}\right)}{\sum_{t=1}^{N_i} m_{v,t}^{obs}} * 100 \tag{3}$$

$$S_i^{temporal} = \frac{\mathrm{var}\left(\tilde{m}_v^{sat}\right)}{\mathrm{var}\left(m_v^{obs}\right)}, \mathrm{var} - \text{variance} \tag{4}$$

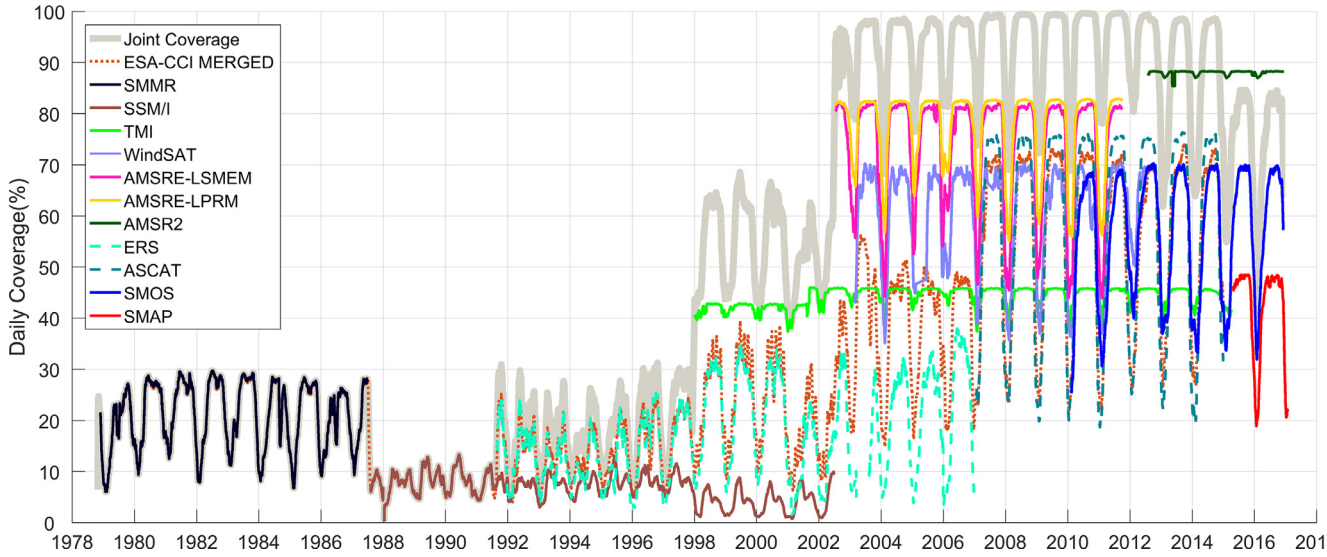

Fig. 2. Time evolution of the daily coverage of passive and active soil moisture products along with their joint coverage. It is observed that the coverage reached maximum (>99%) during 2007–2011, the time period when TMI, AMSR-E, WindSAT, ASCAT, ESA-CCI-COMBI and SMOS (in the later period) have soil moisture retrievals. SMAP along with SMOS is able to cover 85% of the CONUS region during non-winter months.

$$A-RMSE_i^{temporal}=\sqrt{\frac{\sum_{t=1}^{N_i}\left(\left[\tilde{m}_{v,t}^{sat}-\bar{\tilde{m}}_{v,t}^{sat}\right]_i-\left[m_{v,t}^{obs}-\bar{\tilde{m}}_{v,t}^{obs}\right]_i\right)^2}{N_i}},$$

$$\left\{\bar{\tilde{m}}_{v,t}^{d}=\frac{1}{w}\sum_{i=t-(w-1/2)}^{t+(w-1/2)}m_{v,i}^{d}\right\}_{t=1:N_i}^{d=\{obs,sat\}}$$

$$A-R_i^{temporal}=\frac{\mathrm{cov}\left(\tilde{m}_v^{sat}-\bar{\tilde{m}}_v^{sat},\,m_v^{obs}-\bar{m}_v^{obs}\right)}{\sigma_{\tilde{m}_v^{sat}-\bar{\tilde{m}}_v^{sat}}\sigma_{m_v^{obs}-\bar{m}_v^{obs}}} \tag{5}$$

where, w is the width of the moving window. The anomaly time series is computed by removing the seasonal component (computed as a moving average with 'w' as two months i.e., 61 days period) from the actual time series.

$$RMSE_t^{spatial}=\sqrt{\frac{\sum_{i=1}^{\phi}\left(\left[m_{v,i}^{sat}\right]_t-\left[m_{v,i}^{obs}\right]_t\right)^2}{\phi}}$$

$$R_t^{spatial}=\frac{\sum_{i=1}^{\phi}\left(\left[m_{v,i}^{sat}\right]_t-\left[m_{v,mean}^{sat}\right]_t\right)\left(\left[m_{v,i}^{obs}\right]_t-\left[m_{v,mean}^{obs}\right]_t\right)}{\sqrt{\sum_{i=1}^{\phi}\left(\left[m_{v,i}^{sat}\right]_t-\left[m_{v,mean}^{sat}\right]_t\right)^2\sum_{i=1}^{\phi}\left(\left[m_{v,i}^{obs}\right]_t-\left[m_{v,mean}^{obs}\right]_t\right)^2}} \tag{6}$$

3. Results and discussion

3.1. Coverage

Over the past four decades, the daily coverage of microwave sensors has improved significantly over the CONUS (Fig. 2) region. There is an improvement in daily coverage from 30% (during SMMR) to almost 88% (during AMSR-2). The joint coverage follows this pattern, with a peak value greater than 99% during 2007–2011 due to the coexistence of multiple sensors (TMI, AMSR-E, WindSAT, ASCAT and SMOS). SSM/I provided relatively low coverage due to the fact that its retrievals are obtained from a higher frequency (19.3 GHz) that has significant vegetation and atmospheric attenuation. This highlights the importance of having microwave measurements in a low frequency channel for soil moisture retrievals. An increase in coverage by about 3% can be observed from TMI retrievals during 2001 which is due to the satellite orbital boost maneuver made then. In case of active sensors, the ERS satellites have provided limited coverage (<40%) till 2006 which is almost same as that of SMMR. With the launch of ASCAT, which has a dual swath configuration, the coverage almost doubled over ERS. The advent of AMSR-E and WindSAT sensors – that attained global coverage with two overpasses in a day – resulted in an increase in coverage to as high as 82%. AMSR-2 has achieved the highest coverage due to the fact that the associated retrieval algorithm does not filter unreliable retrievals in periods of frozen soil, snow and heavy rainfall conditions. In case of the ESA-CCI-COMBI product, it is found that the process of merging (particularly during the period 1992–2014) does not envelope the coverage of individual products involved in the merging process (contrary to what has been observed in the joint coverage plot). When it comes to dedicated soil moisture missions SMOS and SMAP, the retrievals are carried out using L-band radiometer that varies in their revisit time from 1–3 days, which result in a slight dip in coverage. However, this decrease in coverage comes with an increase in soil and vegetation emission depth, increasing the representative volume of the observations. Furthermore, it can be seen that the coverage time series of all the product follow a seasonal pattern, due to the impact of snow cover and frozen ground over the CONUS. Since the SMAP processor employs a stringent snow cover and frozen ground filtering, the dip in its coverage during the winter of 2016 is much prominent. It can be noticed that the SMAP satellite has lesser daily coverage compared to the coverage of the SMOS satellite. This is due to the fact that there is not much improvement in the daily coverage due to the new inclusion of the ascending pass soil moisture retrievals in the Level 3 *Version 4* SMAP product (result not shown here). Hence, the coverage of the SMAP retrievals presented here mostly correspond to a single (descending) pass, which is not the case with the SMOS retrievals.

3.2. Validation with ISMN station data (m_v^{obs})

3.2.1. Temporal validation

Since soil moisture retrievals are made with different sensors involving different algorithms, it is important to assess their retrievals against reference soil moisture dataset – i.e. up-scaled station values. Fig. 3 shows the boxplots of $RMSE^{temporal}$ and $R^{temporal}$ computed across all the stations for locations with more than 20 simultaneous satellite and in-situ observations. Table 2 presents the median values of $RMSE^{temporal}$, $R^{temporal}$, $B^{temporal}$, $S^{temporal}$, $A-RMSE^{temporal}$ and $A-R^{temporal}$ computed over the CONUS and its

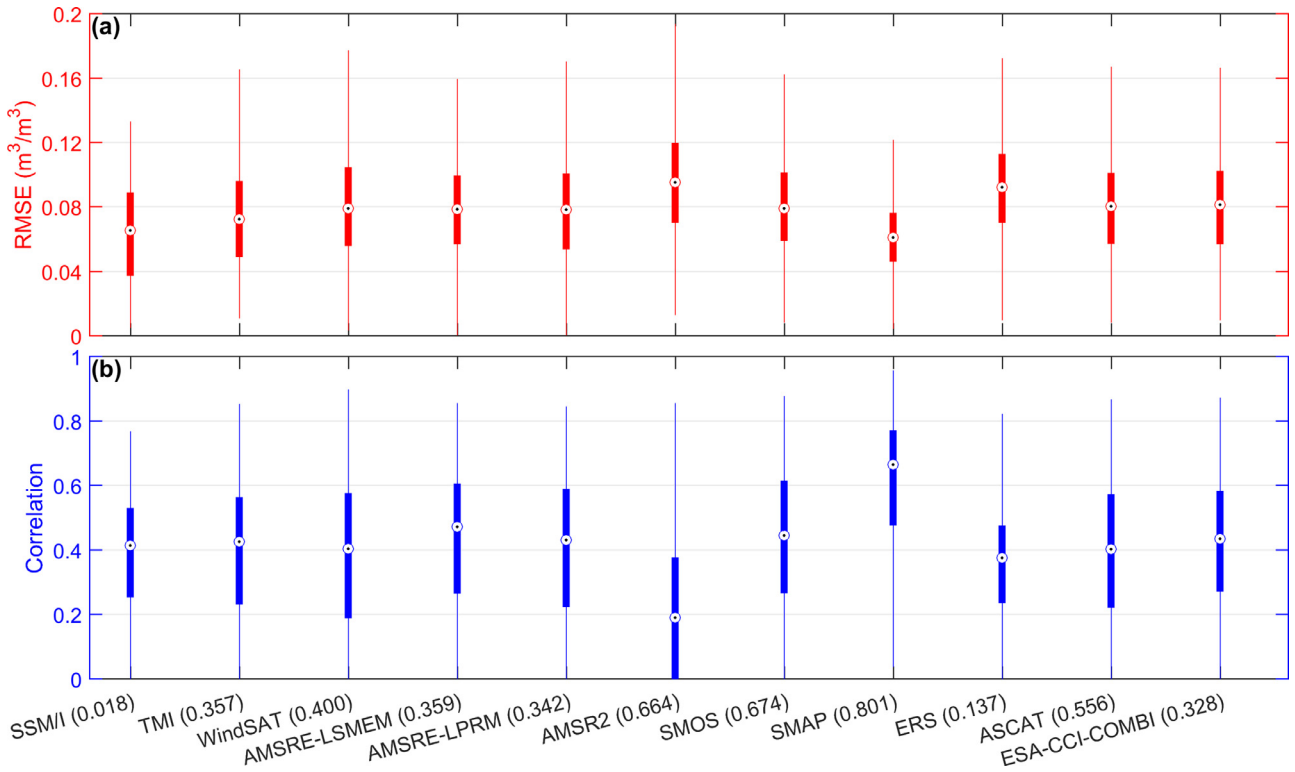

Fig. 3. (a) Temporal *RMSE* ($RMSE^{temporal}$) and (b) Temporal correlation ($R^{temporal}$), of passive and active soil moisture products with respect to m_v^{obs}. Retrieval Validation ratios are provided in the *x*-axis labels and indicate the ratio between the number of retrievals used for validation and total number of retrievals made during the sensor's lifetime.

Table 2
Summary of temporal validation of soil moisture products with m_v^{obs}. Note that the *western* CONUS, the *central* CONUS, and the *eastern* CONUS regions are validated at 510, 96 and 130 grid cells respectively.

	Product	CONUS						Western CONUS					
		RMSE	*R*	*Bias*	*Scale*	*A-RMSE*	*A-R*	*RMSE*	*R*	*Bias*	*Scale*	*A-RMSE*	*A-R*
Temporal Validation with ISMN Soil Moisture	**SMMR**	–	–	–	–	–	–	–	–	–	–	–	–
	SSM/I	0.066	0.41	18.2	2.23	0.112	0.42	0.097	0.39	46.2	1.36	0.094	0.43
	TMI	0.072	0.43	41.7	1.41	0.072	0.24	0.078	0.31	40.9	1.19	0.068	0.23
	WindSAT	0.077	0.42	92.3	1.18	0.070	0.28	0.086	0.33	96.9	1.01	0.067	0.27
	AMSRE-LSMEM	0.079	0.47	−12.9	1.22	0.065	0.33	0.085	0.41	−17.9	1.06	0.067	0.28
	AMSRE-LPRM	0.078	0.43	56.1	1.28	0.069	0.29	0.085	0.36	57.6	1.09	0.066	0.27
	AMSR2	0.095	0.19	−56.4	0.28	0.045	0.29	0.1	0.1	−57.1	0.2	0.041	0.29
	SMOS	0.079	0.45	−30.7	1.02	0.063	0.40	0.087	0.38	−36.3	0.96	0.062	0.37
	SMAP	0.061	0.67	−13.8	0.67	0.044	0.62	0.065	0.62	−23.9	0.61	0.045	0.58
	ERS	0.092	0.38	*	*	*	0.38	0.102	0.34	*	*	*	0.36
	ASCAT	0.081	0.4	*	*	*	0.39	0.085	0.36	*	*	*	0.35
	ESA-CCI-COMBI	0.082	0.44	6.2	0.74	0.055	0.39	0.084	0.41	12.6	0.76	0.060	0.34
	Product	Central CONUS						Eastern CONUS					
		RMSE	*R*	*Bias*	*Scale*	*A-RMSE*	*A-R*	*RMSE*	*R*	*Bias*	*Scale*	*A-RMSE*	*A-R*
	SMMR	–	–	–	–	–	–	–	–	–	–	–	–
	SSM/I	0.041	0.44	−10	5.07	0.114	0.47	0.081	0.42	113.2	2.7	0.116	0.42
	TMI	0.055	0.51	18.8	1.44	0.061	0.38	0.078	0.51	61.4	1.97	0.087	0.21
	WindSAT	0.058	0.51	55.3	1.21	0.061	0.34	0.079	0.52	106.8	1.76	0.088	0.26
	AMSRE-LSMEM	0.057	0.55	−22.3	1.69	0.063	0.51	0.078	0.56	5.3	1.84	0.064	0.40
	AMSRE-LPRM	0.057	0.54	24	1.39	0.063	0.41	0.074	0.54	72.6	2.12	0.086	0.28
	AMSR2	0.082	0.33	−55.6	0.53	0.045	0.41	0.09	0.27	−54.7	0.8	0.067	0.22
	SMOS	0.057	0.67	−21.4	1.1	0.054	0.59	0.075	0.53	−17.6	1.27	0.079	0.35
	SMAP	0.051	0.75	−22.7	0.86	0.043	0.74	0.053	0.77	15	0.82	0.044	0.70
	ERS	0.047	0.52	*	*	*	0.53	0.083	0.41	*	*	*	0.41
	ASCAT	0.062	0.51	*	*	*	0.52	0.08	0.41	*	*	*	0.44
	ESA-CCI-COMBI	0.058	0.54	−8.6	0.76	0.043	0.53	0.084	0.4	0	0.65	0.050	0.42

* The performance metrics could not be computed due to difference in the measurement units of active and reference soil moisture datasets.

three sub-regions (the *western* CONUS, the *central* CONUS, and the *eastern CONUS*). Due to the filtering of stations with low record lengths, SMMR retrievals could not be validated. The results are observed to be influenced chiefly by two important factors, 1) sensor characteristics and retrieval algorithm; and 2) number of stations and the associated total number of observations used for computing the performance metrics. The summary statistics in the table indicate that in general, the *central* CONUS has better soil moisture retrievals which is expected due to the low vegetation in this region. The *western* and *eastern* regions, which are either heavily vegetated or have complex topography show a lower temporal accuracy. It should be noted that the *western* CONUS is validated at a larger number of grid cells (510) compared to the other two regions (96 and 130 for the *eastern* CONUS and *western* CONUS respectively). The effect of record length is quantified for each product by computing the Retrieval Validation ratio (RV_{ratio}) between the number of retrievals compared to station data and the total number of retrievals produced by that product during its life time (at locations where station data is available). A higher value of RV_{ratio} indicates a larger number of retrievals available for the validation, which means that one can have more confidence over the computed performance metrics, and vice versa.

Results from the boxplots indicate that SSM/I product has been validated with the lowest number of observations (low RV_{ratio}), which makes its result less reliable compared to the performance of other products. If we look at the performance of TMI, WindSAT, and AMSRE-LPRM, the RV_{ratio} values are comparable when the retrievals are made using the LPRM algorithm. Thus, all observed differences in their performance are attributable to the respective sensor configurations. The bias ($B^{temporal}$) values of these three products indicate that in general, the LPRM produces wet bias in its soil moisture retrievals. The effect of the change in retrieval algorithm is evident from the results of AMSRE-LSMEM, which resulted in dry bias (contrary to what has been observed in the LPRM results). This bias could have resulted due to changes in the parameterizations, estimation of ancillary surface temperature and vegetation optical depth variables, and the inherent assumptions involved in the two retrieval algorithms. The over estimation of soil moisture made by LPRM is also reported in other studies (Champagne et al., 2010; Peng et al., 2015). Considering scaling errors, it is found that except AMSR2 and SMAP, all the passive products have produced the retrievals with greater variability than that of the station data. The $A-R^{temporal}$ values are lesser than the $R^{temporal}$ for all the products across the CONUS and its regions. This shows that all the products have greater ability in estimating the seasonal variations of soil moisture than its daily variability. In general, lower $A-RMSE^{temporal}$ values are obtained in the *central* CONUS compared to *eastern* and *western* regions. This could be due to the reduced effect of vegetation, which improves (by reducing the effect of canopy) the soil response to instantaneous rainfall in this region. In case of the active products, the retrieval accuracy of ERS is lower (and the metrics are also less reliable because of low RV_{ratio}), which could be due to the coarser temporal and spatial resolutions of the sensor. Since these aspects have been addressed by the ASCAT sensor, it should have boosted the sensor's temporal performance when compared to the ERS product, in terms of an improvement in the median values of $RMSE^{temporal}$ from 0.092 m^3/m^3 to 0.081 m^3/m^3 and $R^{temporal}$ from 0.38 to 0.4 (Table 2) over the CONUS. Due to an increased attention towards soil moisture studies and with the launch of SMOS, AMSR2, and SMAP, the number of stations has increased drastically that improved the RV_{ratio} for these products, which made their validation metrics much more reliable. The weaker performance of AMSR2 in terms of $RMSE^{temporal}$ and $R^{temporal}$ could be more likely due to lack of filtering in the winter periods, since Parinussa et al. (2015) have concluded that the sensor has comparable accuracy with that of AMSR-E when their soil moisture products are retrieved using LPRM algorithm (that has filtered the effects frozen ground and snow). Furthermore, the low $A-RMSE^{temporal}$ achieved by AMSR2 could be related to the reduced variability of the soil moisture retrievals compared to the in-situ observations, which is also supported by the product's low correlation skill and scaling error in the CONUS and its regions. The temporal performance of ESA-CCI-COMBI product is found to be comparable to other products.

Fig. 4 presents the temporal cross correlations between m_v^{sat}, m_v^{obs} and m_v^{VIC}. The cross correlations between any two datasets are computed as the median value of temporal cross correlations obtained across all possible grid locations. It is observed that TMI, WindSAT and AMSR-E-LPRM have high cross-correlations among them. This could be due to a) the same frequency (X-band) used for soil moisture retrievals, b) use of the same retrieval algorithm (LPRM) in case of TMI, WindSAT, and AMSRE-LPRM products, and c) long overlap time (~10 years). The low coverage of the TMI product (Fig. 2) is found to have not affected the cross correlations with other products. In the context of these three products (TMI, WindSAT, and AMSRE-LPRM), the anomaly errors (which quantify the level of agreement between high frequencies across the two datasets) could correspond to the changes occurring in the brightness temperature information due to differences in the sensor configurations, since the retrieval algorithm being used among these products remains the same. Barring few exceptions, the AMSRE-LPRM retrievals have low $A-RMSE^{temporal}$ and high $A-R^{temporal}$ over the CONUS and its sub-regions, which indicates that the AMSR-E's sensor observations are more suitable for the soil moisture retrieval process compared to the sensor observations of TMI and WindSAT, over the CONUS. Despite the use of LPRM algorithm, the results from SSM/I cannot be evaluated along with the aforementioned products. Since, the SSM/I retrievals – developed using 18.7 GHz channel brightness temperature data – are extracted from the ESA-CCI combined passive soil moisture product, there could be effects of channel frequency, and procedure of merging on the retrievals (the SSM/I data is generated as a summation of AMSR-E seasonality and SSM/I anomalies, which are CDF matched with AMSR-E anomalies (Liu et al., 2012)), due to which the anomaly errors may not exclusively correspond to the effect of sensor configuration as was the case with TMI, WindSAT, and AMSRE-LPRM retrievals.

The cross correlation computed between AMSRE-LSMEM and AMSRE-LPRM (the datasets that are derived from same sensor data but different retrieval algorithms) is high. Given this outcome, we can speculate that the low frequency (seasonal) information in the soil moisture retrieval is being more influenced by the instrument configuration and the higher frequencies (daily) are being more influenced by the formulation of the retrieval algorithm. Hence, AMSRE-LSMEM's retrievals producing better $A-R^{temporal}$ over AMSRE-LPRM is an indication that it could better capture the fast component of the soil moisture dynamics over the CONUS region. These results indicate that the noticeable effect of switching between the retrieval algorithms using the same sensor is only observed in terms of bias and anomaly errors (as seen in Fig. 3 and Table 2). SMAP and SMOS, due to the usage of same L-band radiometer based data, are well correlated with each other. Interestingly, though AMSR2 is not well correlated with the ISMN data, it has a reasonable correlation (0.52) with the SMAP product. This clearly indicates that the quality of the soil moisture retrievals is affected by not implementing the filter for the frozen ground and the snow conditions during the winter periods (given that the SMAP processor applied stringent filtering on these conditions). Since SMMR and SSM/I are obtained from the ESA-CCI passive product and, ERS and ASCAT are derived from the ESA-CCI active product, they are found to be highly correlated with

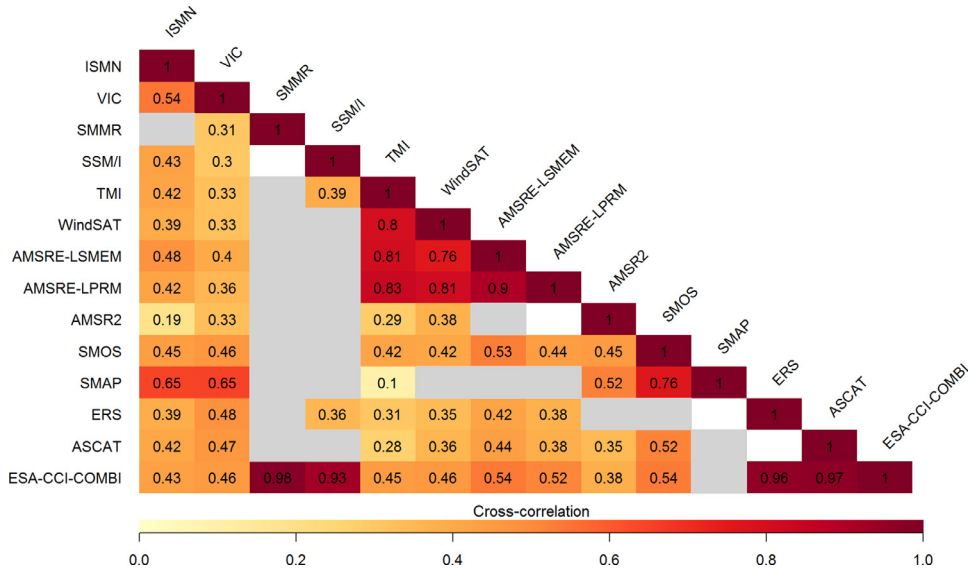

Fig. 4. Cross-correlation between remote sensing products, ISMN data, and VIC-SM. Note that the grey boxes indicate situations when the cross-correlation could not be computed due to non-overlapping sensor operation periods. The cross-correlations are computed with raw data that is not bias corrected, hence, the values could deviate slightly from the other temporal correlation results shown in this paper.

ESA-CCI-COMBI dataset. Interestingly, despite the use of LPRM algorithm, ESA-CCI-COMBI is found to have lesser correlations with TMI, WindSAT and AMSRE-LPRM products. This again signifies the impact of the merging algorithm implemented in this product to obtain long term soil moisture information.

If we look at the performance of the dedicated operational soil moisture missions, it can be noted that SMAP yielded better accuracy, and SMOS resulted in a slightly lower accuracy, which is comparable to AMSR-E and ASCAT. It can be said that the SMAP mission has improved its instrument design based on the experience gained from the SMOS mission regarding its issues with RFI and interferometer design, which could have resulted in an improved accuracy. In addition, the retrieval algorithms used in these products may have also contributed to the difference. Although SMAP has achieved its target accuracy of 0.04 m^3/m^3 at core validation sites spread across the world (Colliander et al., 2017), in the current analysis that is heavily weighted towards sparse networks (i.e. presence of single station per retrieval grid) and stringent filtering of poor quality stations, we find that the retrievals, which have an overall *RMSE* of 0.061 m^3/m^3, have acceptable accuracy. It has been reported that the validation of satellite soil moisture using spare networks indeed inflates the error calculation (due to the gap in spatial representativeness between grid and probes) compared to validation using dense networks i.e. core validation sites (Chen et al., 2016). Compared to SMOS, SMAP's temporal correlations are much closer to each other across the three regions (Table 2). This could mean that SMAP has lesser impact of vegetation dynamics over the CONUS. Also, SMAP is mostly found to have the highest values of $R^{temporal}$ and $A - R^{temporal}$, indicating it is able to capture seasonal as well as daily (high frequency) soil moisture variations accurately. Furthermore, the performance improvement (under increased coverage and RV_{ratio}, which implies an increased robustness in the validation of retrievals pertaining to dedicated soil moisture missions) depicts the success of the community in learning from early missions to improve sensor capabilities as well as retrieval algorithms.

3.2.2. Spatial validation

The evolution of $RMSE^{spatial}$ and $R^{spatial}$ of soil moisture metrics is presented in Fig. 5. Table 3 presents the summary statistics of spatial validation with m_v^{obs} in the three sub-regions and the CONUS. Since the cases of low number of observations/retrievals (<20) are screened, the spatial validation of the SMMR and the SSM/I products could not be carried out. The spatial performance indicates a seasonal cycle with a drop in *RMSE* and an increase in correlation during many of the winter periods. Since the products, including the ESA-CCI-COMBI product, are filtered for frozen soils and snow, the number of uncertain retrievals are reduced, which leaves out the regions of low vegetation during this period, resulting in the reduction of both, the spatial variability of soil moisture and retrieval errors. Moreover, the thin vegetation during the winter months could also contribute (by creating ideal conditions for the soil moisture retrieval) to the better performance of the products in these periods. The strong seasonal cycle is supported by the high correlations (>0.7 over the CONUS) observed in Table 3. This situation is reversed in the case of AMSR2 i.e., higher errors during some of the winter months (for example starting of 2016 in the figure). This could be because the AMSR2 processor does not filter for the effects of snow and frozen ground conditions. Nonetheless, all the soil moisture products have retrievals with reasonable accuracy given that none of the stations used for the analysis have been filtered – leading to the evaluation for all weather, vegetation, soil properties and topographic conditions. However, it is important to look at these plots in conjunction with Fig. 1(b) that shows the growth in station numbers over time. It is always desirable for a product to perform well across a large number of stations. It is noted that the $RMSE^{spatial}$ on a particular day is inherently dependent on the number of available in-situ values. So, a reduction in the number of stations, could by chance result in smaller errors. This is evident from the performance of TMI, ERS and ESA-CCI-COMBI products, which have smaller $RMSE^{spatial}$ and $R^{spatial}$ for retrievals made prior to 2003, a period that has a lower number of ground observations available for validation (see Fig 1b). Furthermore, The TMI product has reasonably high $R^{spatial}$ throughout its history, which indicates that the product's seasonal dynamics agree well with the ISMN data.

The $R^{spatial}$ of soil moisture products (Table 3) is found to be greater than the products' temporal correlation (Table 2). This could mean that all of the products, despite their variations in sensor configurations and retrieval algorithms, are able to produce reasonably accurate spatial patterns of soil moisture. The spatial performance of the products in recent years indicates a slight de-

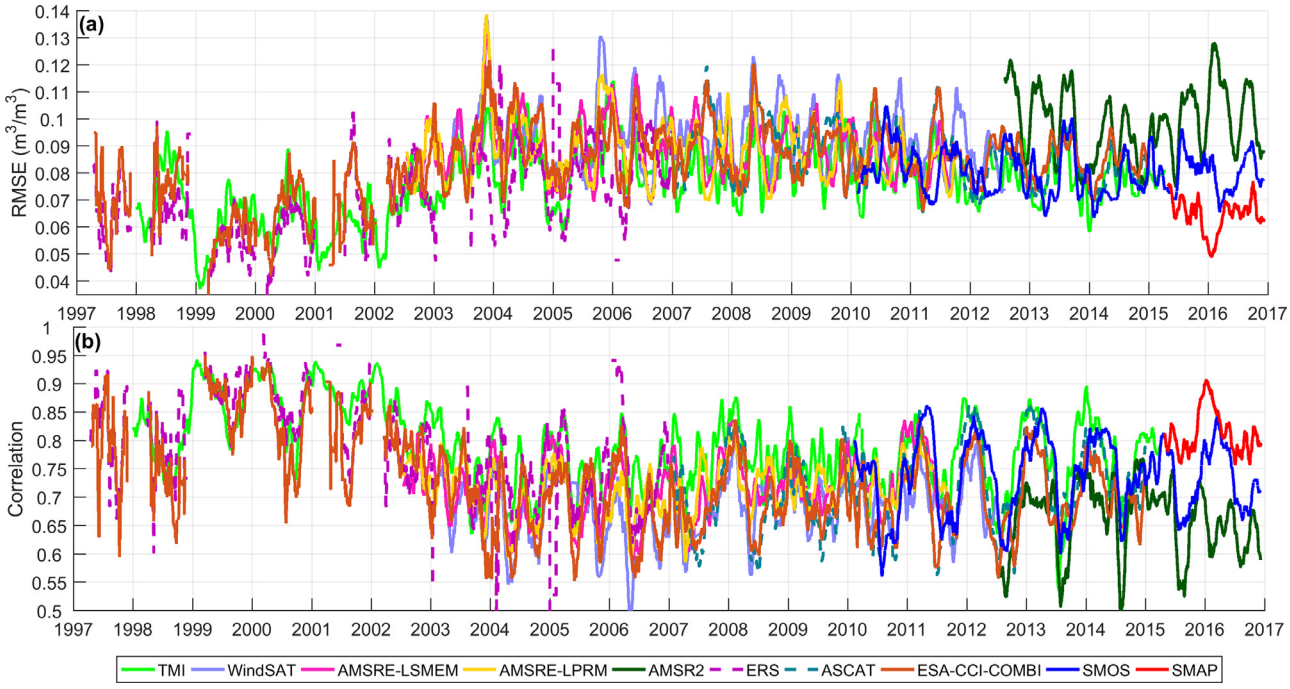

Fig. 5. (a) Spatial *RMSE* ($RMSE^{spatial}$) and (b) Spatial correlation ($R^{spatial}$), of passive and active soil moisture products with respect to the ISMN data (m_v^{obs}).

Table 3
Summary of spatial validation of soil moisture products with ISMN soil moisture (m_v^{obs}). Note that the *western* CONUS, the *central* CONUS, and the *eastern* CONUS regions are validated at 510, 96 and 130 grid cells respectively. SMMR and SSM/I could not be validated due to low availability of observations/retrievals (fewer than 20) for validation.

Product	Spatial validation with ISMN soil moisture							
	CONUS		Western CONUS		Central CONUS		Eastern CONUS	
	RMSE	*R*	*RMSE*	*R*	*RMSE*	*R*	*RMSE*	*R*
SMMR	–	–	–	–	–	–	–	–
SSM/I	–	–	–	–	–	–	–	–
TMI	0.076	0.80	0.09	0.64	0.051	0.90	0.073	0.82
WindSAT	0.084	0.72	0.101	0.59	0.056	0.87	0.079	0.73
AMSRE-LSMEM	0.086	0.72	0.094	0.61	0.051	0.90	0.081	0.74
AMSRE-LPRM	0.086	0.72	0.098	0.61	0.051	0.90	0.073	0.79
AMSR2	0.099	0.67	0.103	0.59	0.08	0.74	0.09	0.72
SMOS	0.079	0.75	0.082	0.68	0.057	0.83	0.078	0.73
SMAP	0.064	0.82	0.067	0.77	0.053	0.87	0.056	0.84
ERS	0.077	0.77	0.098	0.57	0.048	0.90	0.082	0.71
ASCAT	0.086	0.71	0.091	0.63	0.063	0.82	0.081	0.76
ESA-CCI-COMBI	0.086	0.71	0.093	0.60	0.064	0.81	0.084	0.73

terioration in the results. This could be due to the fact that since 2010, out of 334 grid locations where new stations have been setup over the CONUS, 255 grid cells lie in the *western* CONUS region, whose complex topography and presence of dense forests might have affected the overall spatial performance assessment of the products (except SMAP) since 2010. This is evident from the lower accuracy of products in the *western* CONUS region (Table 3). However, SMAP, even here, is found to be less affected by these effects compared to other products. This signifies the advancements that the sensor underwent with the knowledge learned from SMOS as well as the other past missions. Despite discontinuities due to low temporal resolution along with coarse spatial resolution, the $RMSE^{spatial}$ and $R^{spatial}$ of the ERS retrievals are better than that of ASCAT, which is contrary to what has been found in the case of temporal analysis. There seems to be a minimal effect of the retrieval algorithm on the spatial characteristics of AMSRE-LSMEM and AMSRE-LPRM. The soil moisture satellites SMOS and SMAP have performed exceptionally well in maintaining *RMSEs* in the ranges of 0.07–0.09 and 0.06–0.07 m^3/m^3 respectively during non-winter periods using ~1000 in-situ stations. The effect of filtering for frozen soils and snow is much prominent in the SMAP performance (the low coverage (<20%) during 2016 period of SMAP can be seen in Fig. 2).

3.3. Validation with the VIC land surface model soil moisture (m_v^{VIC})

3.3.1. Temporal validation

Since the above validation study is constrained to locations where the ISMN data are available, we compared the soil moisture products with simulations from the VIC-SM (m_v^{VIC}). The model simulations are available for the period 1979-present, which makes it possible to compute spatial and temporal performance metrics across all grid cells over the CONUS. Prior to this comparison, the model was compared with the ISMN data where it performed with reasonable accuracy. Results are presented in supplementary material S1. Table 4 presents the summary statistics of temporal performance of the soil moisture products. The scale errors ($S^{temporal}$) indicate that the VIC-SM produces soil moisture simulations with

Table 4
Summary statistics of temporal validation of soil moisture products with m_v^{VIC}.

	Product	CONUS						Western CONUS					
		RMSE	*R*	*Bias*	*Scale*	*A-RMSE*	*A-R*	*RMSE*	*R*	*Bias*	*Scale*	*A-RMSE*	*A-R*
Temporal validation with VIC soil moisture	**SMMR**	0.034	0.31	6.9	3.93	0.110	0.30	0.032	0.53	6.9	3.93	0.085	0.53
	SSM/I	0.034	0.29	−7.3	3.57	0.086	0.30	0.035	0.40	6.5	4.07	0.072	0.40
	TMI	0.033	0.32	4.6	3.41	0.066	0.31	0.030	0.53	9.3	4.18	0.051	0.42
	WindSAT	0.033	0.32	33.1	3.28	0.066	0.35	0.030	0.53	16.4	3.74	0.047	0.45
	AMSRE-LSMEM	0.035	0.39	−25.2	3.97	0.061	0.49	0.030	0.57	−7.9	3.82	0.054	0.54
	AMSRE-LPRM	0.032	0.35	13.3	3.66	0.066	0.41	0.030	0.57	8.3	3.80	0.047	0.50
	AMSR2	0.033	0.30	−69.9	1.37	0.034	0.36	0.037	0.30	−14.2	3.46	0.019	0.43
	SMOS	0.031	0.44	−50.7	2.84	0.062	0.42	0.035	0.46	−12.7	3.56	0.053	0.48
	SMAP	0.026	0.65	−32.5	1.92	0.037	0.64	0.026	0.72	−5.6	3.48	0.030	0.67
	ERS	0.030	0.45	*	*	*	0.48	0.039	0.41	*	*	*	0.48
	ASCAT	0.031	0.44	*	*	*	0.44	0.040	0.41	*	*	*	0.43
	ESA-CCI-COMBI	0.031	0.45	−25.0	1.80	0.043	0.45	0.034	0.50	−5.3	3.44	0.044	0.49
	Product	Central CONUS						Eastern CONUS					
		RMSE	*R*	*Bias*	*Scale*	*A-RMSE*	*A-R*	*RMSE*	*R*	*Bias*	*Scale*	*A-RMSE*	*A-R*
	SMMR	0.030	0.33	−10.5	3.72	0.095	0.30	0.036	0.16	53.7	6.02	0.165	0.17
	SSM/I	0.031	0.26	−8.1	3.90	0.086	0.26	0.035	0.22	22.8	5.23	0.121	0.22
	TMI	0.031	0.36	−22.0	3.18	0.057	0.42	0.036	0.19	44.1	6.08	0.095	0.15
	WindSAT	0.030	0.32	15.1	3.09	0.057	0.38	0.036	0.19	90.1	5.61	0.095	0.18
	AMSRE-LSMEM	0.030	0.37	−33.9	4.19	0.064	0.54	0.047	0.23	−6.9	5.80	0.063	0.29
	AMSRE-LPRM	0.030	0.33	−2.6	3.47	0.059	0.45	0.035	0.19	51.9	6.52	0.093	0.21
	AMSR2	0.027	0.42	−70.5	1.37	0.029	0.39	0.033	0.26	−64.0	2.14	0.051	0.27
	SMOS	0.026	0.52	−46.6	2.85	0.057	0.49	0.031	0.29	−36.0	3.72	0.083	0.20
	SMAP	0.021	0.65	−43.5	2.30	0.043	0.67	0.027	0.53	9.1	2.09	0.040	0.54
	ERS	0.026	0.50	*	*	*	0.50	0.028	0.45	*	*	*	0.45
	ASCAT	0.028	0.46	*	*	*	0.47	0.029	0.45	*	*	*	0.45
	ESA-CCI-COMBI	0.028	0.43	−33.4	1.86	0.039	0.46	0.030	0.41	−12.4	1.84	0.043	0.40

* The performance metrics could not be computed due to difference in the measurement units of active and reference soil moisture datasets.

lower variability than the station soil moisture, resulting in significant scaling differences. This occurs due to two reasons (related to the model parameterizations), 1) the top soil layer loses moisture only through gravity drainage and such drainage basically stops around half saturation; and 2) no under-canopy (or between-plant) soil evaporation is parameterized to further dry down the soil when gravity drainage stops (Pan et al., 2014). The $RMSE^{temporal}$ computed between the soil moisture products and m_v^{VIC} is found to be better than that of the ISMN data (Table 2) for all the products in the CONUS and its regions. Such low values of $RMSE^{temporal}$ are expected due to the low temporal variability of the VIC-SM, whose median value of standard deviations over the CONUS is found to be 0.028 m^3/m^3 (for reference, a histogram plot of standard deviations over the CONUS is presented in supplementary material S2). Entekhabi et al. (2010b) have deduced that *RMSE* values less than the target *RMSE* can be achieved, given the standard deviation of the reference soil moisture to be less than the target *RMSE* value, which has happened in the current case (all $RMSE^{temporal}$ values are less than the desired target of 0.04 m^3/m^3). In this regard, the correlation metric shall provide the true strength of the relationship between satellite data and the VIC-SM. Interestingly, the products have obtained lower $R^{temporal}$ values during the VIC model based validation, compared to the $R^{temporal}$ values of the ISMN based validation (see Table 2). This could indicate that the satellite products have produced better soil moisture retrievals than the model simulations over the CONUS. In the case of anomaly errors, the VIC model based validation mostly produced better $A - R^{temporal}$ values. This means that there is good agreement between the daily variabilities of satellite and the VIC model soil moisture in these regions. This could be due to the fact that the VIC model estimates the soil moisture (as a state variable) using the forcing data at daily scale (along with other variables), thus being sensitive to the high frequency variability of precipitation. In addition, both VIC model and the retrieval algorithms of most sensors use soil data derived from common soil products that could impact the simulation of the soil moisture dynamics. Even under this validation, the anomaly errors indicate that, in case of sensors, AMSR-E produced accurate brightness temperatures compared to TMI and WindSAT, and in case of retrieval algorithm, AMSRE-LSMEM produced accurate soil moisture retrievals when compared with AMSRE-LPRM. The accuracy of retrievals from ESA-CCI-COMBI product is found to be at par with other products, but with a negative $B^{temporal}$. Since the merging process involves bias correcting (CDF matching) the active and passive soil moisture products with Noah land surface model soil moisture simulations, the values of which are found to be lower than the VIC-SM over the CONUS (Liu et al., 2012), it would have resulted in the negative bias.

The maps of $R^{temporal}$ and $RMSE^{temporal}$ of the soil moisture missions SMOS and SMAP are presented in Fig. 6 (a, b) and Fig. 6 (c, d) respectively. Results for the other sensors are available in the supplementary material S3. SMOS and SMAP have retrieved soil moisture with median $RMSE^{temporal}$ of 0.031 m^3/m^3 and 0.026 m^3/m^3 and $R^{temporal}$ of 0.44 and 0.65 respectively. The error pattern of SMOS is more aligned with vegetation and topography of the CONUS, for example, higher errors are found in the dense forests and topographically complex terrains of the Sierra Nevada and portions of the Rocky Mountains. Such effects are less prominent in case of SMAP. The difference could be due to the fact that the SMOS processor separately addresses the effect of forests in its retrieval algorithm, which is not the case with SMAP resulting in identifiable spatial features in the error maps of SMOS. Moreover, the improved instrument design of SMAP could have limited its requirement to a simpler algorithm (Single Channel Algorithm) to retrieve soil moisture under all land cover conditions. Remarkably, both the products have produced low $RMSE^{temporal}$ with the VIC-SM in the forested regions of the *eastern* CONUS (also seen from Table 4) which are considered challenging due to the attenuation of vegetation. Interestingly, it can be seen from Fig. 4 that ASCAT

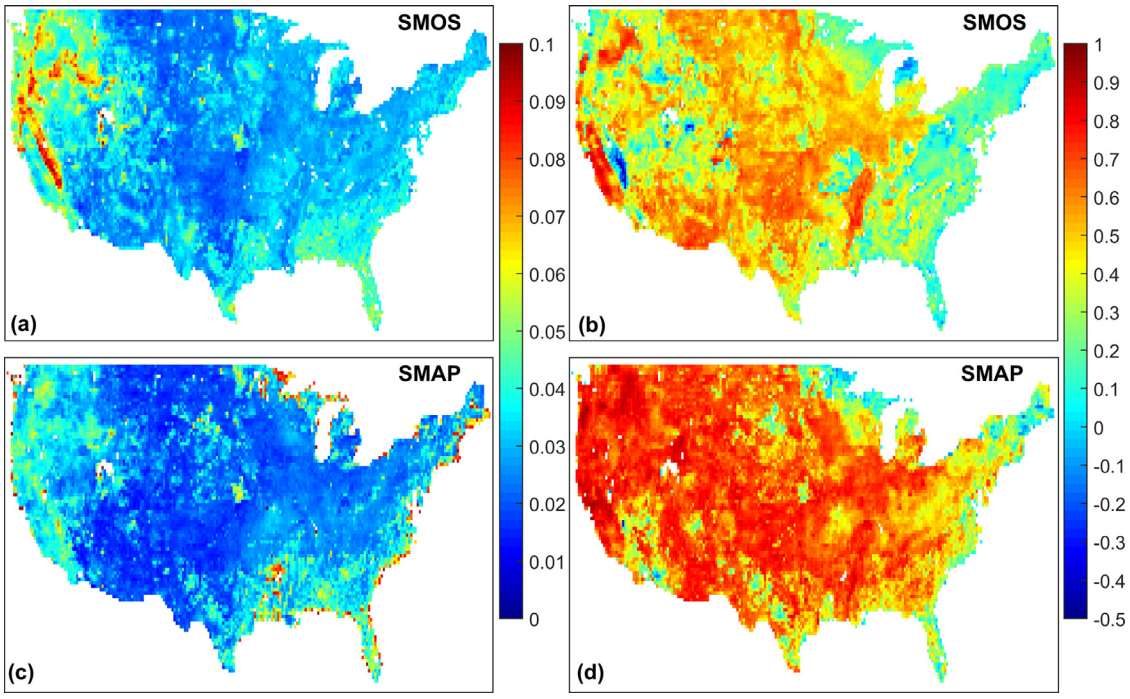

Fig. 6. Maps of (a) Temporal *RMSE* ($RMSE^{temporal}$) of SMOS; (b) Temporal correlation ($R^{temporal}$) of SMOS; (c) Temporal *RMSE* ($RMSE^{temporal}$) of SMAP; (d) Temporal correlation ($R^{temporal}$) of SMAP. These metrics are computed with m_v^{VIC} as reference over the CONUS.

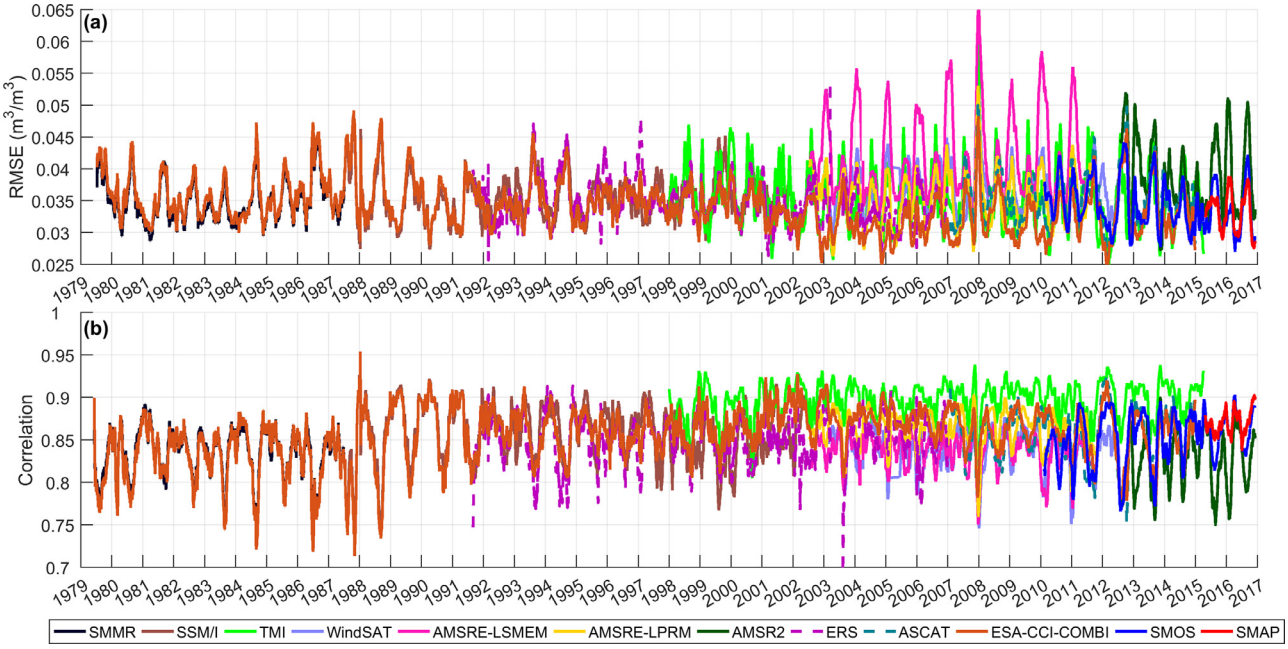

Fig. 7. (a) Spatial *RMSE* ($RMSE^{spatial}$) and (b) Spatial correlation ($R^{spatial}$), of passive and active soil moisture products with respect to the VIC-SM (m_v^{VIC}).

has reasonably high correlation (0.52) with the SMOS product despite the contrasting differences in sensor type and retrieval algorithm. If we look at this result in tandem with the temporal performance of these products, it can be said that the ASCAT retrieved soil moisture with similar accuracy as that of the SMOS product. This result is in agreement with study carried out by Al-Yaari et al., (2014) in comparing the two products with a land surface model.

3.3.2. Spatial validation

The $RMSE^{spatial}$ and $R^{spatial}$ time series for soil moisture products with m_v^{VIC} are presented in Fig. 7. Table 5 presents the summary statistics of spatial validation of all the products with model simulations. The results indicate that in general, all the products have *RMSE*s below 0.05 $m^3/m^3$and correlations above 0.7 across all the regions of the CONUS. The products are noted to have high spatial performance (Table 5) compared to the temporal performance. This observation is consistent with the observation made using the ISMN data based analysis (Section 3.2). From this, it can be said that all the soil moisture products can reproduce the expected spatial dynamics of soil moisture over the CONUS. Furthermore, the spatial performance in the figure indicates a seasonal pattern though it is slightly different from what has been observed in case

Table 5
Summary statistics of spatial validation of soil moisture products with m_v^{VIC}.

Product	Spatial validation with VIC soil moisture							
	CONUS		Western CONUS		Central CONUS		Eastern CONUS	
	RMSE	*R*	*RMSE*	*R*	*RMSE*	*R*	*RMSE*	*R*
SMMR	0.034	0.84	0.036	0.77	0.029	0.89	0.036	0.82
SSM/I	0.035	0.87	0.035	0.84	0.029	0.88	0.037	0.82
TMI	0.034	0.90	0.032	0.87	0.03	0.92	0.036	0.90
WindSAT	0.037	0.85	0.036	0.80	0.03	0.90	0.039	0.84
AMSRE-LSMEM	0.040	0.84	0.036	0.82	0.032	0.90	0.046	0.79
AMSRE-LPRM	0.035	0.87	0.033	0.84	0.031	0.90	0.038	0.86
AMSR2	0.038	0.83	0.044	0.77	0.03	0.88	0.035	0.86
SMOS	0.033	0.86	0.036	0.81	0.029	0.88	0.032	0.86
SMAP	0.033	0.87	0.030	0.86	0.026	0.91	0.036	0.82
ERS	0.034	0.87	0.038	0.79	0.029	0.89	0.031	0.88
ASCAT	0.035	0.86	0.041	0.79	0.03	0.88	0.03	0.89
ESA-CCI-COMBI	0.033	0.87	0.035	0.82	0.029	0.89	0.033	0.87

of ISMN based validation (Fig. 5). Here, the spatial errors are higher during the winter and lower during spring followed by a rise in summer. It is difficult to provide a physical interpretation for this pattern as the spatial errors are computed across all the land cover and climatology regimes of the CONUS. Fig. 7 indicates that the time series of SMAP, and to some extent SMOS, have low amplitude compared to other products. This indicates that despite the seasonal changes, SMOS and SMAP have produced consistent spatial performance throughout the year. In case of AMSR-E, the effect of the two retrieval algorithms is more prominent with AMSRE-LPRM performing better than AMSRE-LSMEM. Even here the spatial performance of ERS product is better than the ASCAT product. However, the performance of ERS and ASCAT retrievals are comparable to that of contemporary passive products. This indicates that the change detection algorithm might have successfully dealt with the impact of roughness on active microwave soil moisture retrievals. The $RMSE^{spatial}$ of all the products – across all the regions, barring few exceptions – are mostly below the desired level of 0.04 m^3/m^3. The spatial performance of soil moisture products when validated with the VIC-SM is found to be better in comparison with the spatial validation using the ISMN data. This could mean that both model simulations and satellite retrievals behaved in similar fashion when it comes to dealing with different biomes and topography conditions. It is important to recognize that satellite soil moisture products have successfully captured the true dynamics of soil moisture, at least over the CONUS.

4. Summary and conclusions

The present work aims to provide a review of what has been achieved over past four decades of satellite microwave remote sensing of soil moisture in terms of sensor performance over the Contiguous United States (CONUS) region. In this process, we evaluated eight passive and two active microwave sensors with respect to the International Soil Moisture Network (ISMN) in-situ measurements and soil moisture simulations derived from the Variable Infiltration Capacity (VIC) model.

Initially, the passive microwave instruments were intended mostly for meteorological applications. Due to the presence of low frequency channels in those instruments, it was possible to retrieve soil moisture thus leading to the development of approximately four decades of global scale soil moisture information. Early missions like SMMR and SSM/I had low spatial and temporal coverage due to power limitations. The launch of AMSE-E and WindSAT significantly improved global coverage. With SMOS and SMAP, the instrument design aimed to achieve good spatial and temporal resolutions along with the use of an L-band radiometer. The active microwave instrument ERS-1 scatterometer started retrieving soil moisture at global scale two decades after the launch of SMMR. Due to sensor limitations, the retrievals were made at low spatial and temporal resolutions. This was improved upon in the succeeding ASCAT missions launched with the MetOp satellites. For any sensor and satellite platform, there is always a trade-off between major design factors like operating frequency (lower frequency for better penetration depth), antenna size (longer wave length requires a larger aperture for the same resolution), payload (cost), orbit height, swath width, and revisit time. Dedicated missions are able to better optimize their configurations, and thus offer a better value for soil moisture related applications.

Our analysis of passive and active microwave soil moisture products over the CONUS region infer the following points:

- The daily coverage of both passive and active sensors has significantly improved in the last four decades. All the products except AMSR2 exhibit seasonal effect with lower number of retrievals made during winter periods, due to filtering of retrievals over frozen ground and snow covered parts of the land surface. ASCAT mission doubled the active microwave retrievals compared to its predecessor. In the overlapping period of TMI, WindSAT, AMSR-E, ASCAT, SMOS, and ESA-CCI-COMBI (2007–2011), a daily coverage of almost 100% could be achieved. The daily coverage has increased from 30% during 1980s to approximately 85% (during non-winter months) with the launch of dedicated operational soil moisture missions SMOS and SMAP.
- The temporal validation of passive and active soil moisture products with the ISMN data place the range of median *RMSE* as 0.06–0.10 m^3/m^3 and median correlation as 0.20–0.68. Despite the absence of filtering for topography and weather conditions, the soil moisture products show a medium to good accuracy in reproducing in-situ soil moisture dynamics observed from the ISMN. The ASCAT product shows a significant improvement during the temporal validation of retrievals compared to its predecessor ERS, thanks to enhanced sensor configuration.
- In terms of comparison of sensors, when TMI, AMSR-E, and WindSAT are evaluated, the AMSR-E sensor is found to have produced the brightness temperatures with better quality, given that these sensors are paired with same retrieval algorithm (LPRM).
- The low performance of AMSR2 in winter signifies the importance of filtering the retrievals for frozen ground and snow conditions. This is supported by the high-correlation of AMSR2 and SMAP which shows that an additional filtering could significantly boost the performance of AMSR2.
- The SMAP mission, through its improved sensor design and RFI handling, shows a high retrieval accuracy under all-topography

conditions. Although the retrievals from the SMOS mission are affected by issues such as RFI, the accuracy is still comparable to or better than that of AMSR-E and ASCAT sensors.
- With the knowledge gained from SMOS, SMAP's design resulted in accuracy that is less impacted by the vegetation conditions and topography over the CONUS.
- All soil moisture products have indicated better agreement with the ISMN data than the VIC-SM, which indicate that they produce soil moisture with better accuracy than the VIC-SM over the CONUS.

5. Future challenges

Based on the results and conclusions obtained through this analysis, we have highlighted below some of the remaining challenges in microwave soil moisture estimates for validation, calibration, and applications:

- Establishing more local dense sensor networks (like SMAP core validation sites), especially in regions with low observation density. This will provide valuable benchmark data for the validation of retrieval algorithms and improvements to sensors and retrieval algorithms.
- Develop robust alternate validation techniques using land surface model derived soil moisture, which can improve our understanding of soil moisture retrieval quality in regions without the need for ground observations. This development can be supported by the use of hyper-resolution land surface models that are able to capture the spatial heterogeneity of the soil moisture at sub-satellite grid resolution (Cai et al., 2017).
- Improve our ability to retrieve soil moisture over densely vegetated regions. In this regard, the possibility of deploying dedicated soil moisture P-band (0.25–0.50 GHz) sensors should be explored.
- Given the four decades of remotely sensed soil moisture observations, the focus should be directed towards creating a harmonized ensemble, multi-algorithm global soil moisture record, which is free from the influences of instrument characteristics and the sensor frequency. This would provide a next step to the current CDF-matching algorithm used to create the ESA-CCI long-term soil moisture record (Liu et al., 2012).

Acknowledgments

The work reported in this paper was done while the first author was a visiting scholar at Princeton University under the Fulbright-Nehru India Doctoral Research program (Grant Id: 15160292). Additional support for the research is from NASA Grants NNX14AH92G (Soil Moisture Cal/Val Activities as a SMAP Mission Science Team Member) and NNX13AI44G (Developing a statistical-physical integrated approach for downscaling hydrologic information from GCM), and NWO Rubicon 825.15.003. The support from these programs is gratefully acknowledged.

Supplementary materials

Supplementary material associated with this article can be found, in the online version, at doi:10.1016/j.advwatres.2017.09.010.

References

Al-Yaari, A., Wigneron, J.-P., Ducharne, A., Kerr, Y., Wagner, W., De Lannoy, G., Reichle, R., Al Bitar, A., Dorigo, W., Richaume, P., 2014. Global-scale comparison of passive (SMOS) and active (ASCAT) satellite based microwave soil moisture retrievals with soil moisture simulations (MERRA-Land). Remote Sens. Environ. 152, 614–626.

Al Bitar, A., Leroux, D., Kerr, Y.H., Merlin, O., Richaume, P., Sahoo, A., Wood, E.F., 2012. Evaluation of SMOS soil moisture products over continental US using the SCAN/SNOTEL network. IEEE Trans. Geosci. Remote Sens. 50, 1572–1586.

Alvarez-Garreton, C., Ryu, D., Western, A.W., Crow, W.T., Su, C.H., Robertson, D.R., 2016. Dual assimilation of satellite soil moisture to improve streamflow prediction in data scarce catchments. Water Resour. Res. 52, 5357–5375.

Bartalis, Z., Wagner, W., Naeimi, V., Hasenauer, S., Scipal, K., Bonekamp, H., Figa, J., Anderson, C., 2007. Initial soil moisture retrievals from the METOPA advanced scatterometer (ASCAT). Geophys. Res. Lett. 34, L20401.

Bindlish, R., Jackson, T.J., Wood, E., Gao, H., Starks, P., Bosch, D., Lakshmi, V., 2003. Soil moisture estimates from TRMM Microwave Imager observations over the Southern United States. Remote Sens. Environ. 85, 507–515.

Botter, G., Peratoner, F., Porporato, A., Rodriguez Iturbe, I., Rinaldo, A., 2007. Signatures of large scale soil moisture dynamics on streamflow statistics across US climate regimes. Water Resour. Res. 43, W11413.

Brodzik, M.J., Billingsley, B., Haran, T., Raup, B., Savoie, M.H., 2012. EASE-Grid 2.0: Incremental but significant improvements for Earth-gridded data sets. ISPRS Int. J. Geo-Inf. 1, 32–45.

Cai, X., Pan, M., Chaney, N.W., Colliander, A., Misra, S., Cosh, M.H., Crow, W.T., Jackson, T.J., Wood, E.F., 2017. Validation of SMAP soil moisture for the SMAPVEX15 field campaign using a hyper resolution model. Water Resour. Res. 53, 3013–3028.

Champagne, C., Berg, A., Belanger, J., McNairn, H., De Jeu, R., 2010. Evaluation of soil moisture derived from passive microwave remote sensing over agricultural sites in Canada using ground-based soil moisture monitoring networks. Int. J. Remote Sens. 31, 3669–3690.

Chan, S.K., Bindlish, R., O'Neill, P.E., Njoku, E., Jackson, T., Colliander, A., Chen, F., Burgin, M., Dunbar, S., Piepmeier, J., 2016. Assessment of the SMAP passive soil moisture product. IEEE Trans. Geosci. Remote Sens. 54, 4994–5007.

Chen, F., Crow, W.T., Colliander, A., Cosh, M.H., Jackson, T.J., Bindlish, R., Reichle, R.H., Chan, S.K., Bosch, D.D., Starks, P.J., 2016. Application of triple collocation in ground-based validation of soil moisture active/passive (SMAP) level 2 data products. IEEE J. Select. Top. Appl. Earth Obs. Remote Sens 10 (2), 489–502.

Colliander, A., Jackson, T., Bindlish, R., Chan, S., Das, N., Kim, S., Cosh, M., Dunbar, R., Dang, L., Pashaian, L., 2017. Validation of SMAP surface soil moisture products with core validation sites. Remote Sens. Environ. 191, 215–231.

Colliander, A., Jackson, T., McNairn, H., Chazanoff, S., Dinardo, S., Latham, B., O'Dwyer, I., Chun, W., Yueh, S., Njoku, E., 2015. Comparison of airborne passive and active L-band system (PALS) brightness temperature measurements to SMOS observations during the SMAP validation experiment 2012 (SMAPVEX12). IEEE Geosci. Remote Sens. Lett. 12, 801–805.

Crapolicchio, R., Lecomte, P., 2004. The ERS-2 scatterometer mission: events and long-loop instrument and data performances assessment. In: Proceedings of the 2004 ENVISAT & ERS Symposium, pp. 6–10.

Crow, W.T., 2007. A novel method for quantifying value in spaceborne soil moisture retrievals. J. Hydrometeorol. 8, 56–67.

Crow, W.T., Miralles, D.G., Cosh, M.H., 2010. A quasi-global evaluation system for satellite-based surface soil moisture retrievals. IEEE Trans. Geosci. Remote Sens. 48, 2516–2527.

Crow, W.T., Ryu, D., Famiglietti, J.S., 2005. Upscaling of field-scale soil moisture measurements using distributed land surface modeling. Adv. Water Res. 28, 1–14.

Crow, W.T., Zhan, X., 2007. Continental-scale evaluation of remotely sensed soil moisture products. IEEE Geosci. Remote Sens. Lett. 4, 451–455.

D'odorico, P., Laio, F., Porporato, A., Rodriguez-Iturbe, I., 2003. Hydrologic controls on soil carbon and nitrogen cycles. II. A case study. Adv. Water Res. 26, 59–70.

De Jeu, R., 2011a. In: GSFC, V.U.A.a.N. (Ed.), LPRM/AMSR-E/Aqua Daily L3 Ascending Surface Soil Moisture, Ancillary Params, and QC. Goddard Earth Sciences Data and Information Services Center (GES DISC), Greenbelt, MD U.S.A.

De Jeu, R., 2011b. In: GSFC, V.U.A.a.N. (Ed.), LPRM/AMSR-E/Aqua Daily L3 Descending Surface Soil Moisture, Ancillary Params, and QC. Goddard Earth Sciences Data and Information Services Center (GES DISC), Greenbelt, MD U.S.A.

De Jeu, R., 2012a. In: GSFC, V.U.A.a.N. (Ed.), LPRM/TMI/TRMM Daily L3 Day Surface Soil Moisture, Ancillary Params, and QC. Goddard Earth Sciences Data and Information Services Center (GES DISC), Greenbelt, MD U.S.A.

De Jeu, R., 2012b. In: GSFC, V.U.A.a.N. (Ed.), LPRM/TMI/TRMM Daily L3 Night Surface Soil Moisture, Ancillary Params, and QC. Goddard Earth Sciences Data and Information Services Center (GES DISC), Greenbelt, MD U.S.A..

De Lannoy, G.J., Reichle, R.H., 2016. Assimilation of SMOS brightness temperatures or soil moisture retrievals into a land surface model. Hydrol. Earth Syst. Sci. 20, 4895.

de Rosnay, P., Balsamo, G., Albergel, C., Muñoz-Sabater, J., Isaksen, L., 2014. Initialisation of land surface variables for numerical weather prediction. Surv. Geophys. 35, 607–621.

Delwart, S., Bouzinac, C., Wursteisen, P., Berger, M., Drinkwater, M., Martín-Neira, M., Kerr, Y.H., 2008. SMOS validation and the COSMOS campaigns. IEEE Trans. Geosci. Remote Sens. 46, 695–704.

Dirmeyer, P.A., Halder, S., 2016. Sensitivity of numerical weather forecasts to initial soil moisture variations in CFSv2. Weather Forecast. 31, 1973–1983.

Dorigo, W., Gruber, A., De Jeu, R., Wagner, W., Stacke, T., Loew, A., Albergel, C., Brocca, L., Chung, D., Parinussa, R., 2015. Evaluation of the ESA CCI soil moisture product using ground-based observations. Remote Sens. Environ. 162, 380–395.

Dorigo, W., Wagner, W., Hohensinn, R., Hahn, S., Paulik, C., Xaver, A., Gruber, A., Drusch, M., Mecklenburg, S., Oevelen, P.v, 2011. The international soil moisture network: a data hosting facility for global in situ soil moisture measurements. Hydrol. Earth Syst. Sci. 15, 1675–1698.

Dorigo, W., Xaver, A., Vreugdenhil, M., Gruber, A., Hegyiová, A., Sanchis-Dufau, A., Zamojski, D., Cordes, C., Wagner, W., Drusch, M., 2013. Global automated quality control of in situ soil moisture data from the international soil moisture network. Vadose Zone J. 12.

Drusch, M., 2007. Initializing numerical weather prediction models with satellite derived surface soil moisture: data assimilation experiments with ECMWF's integrated forecast system and the TMI soil moisture data set. J. Geophys. Res.: Atmosp. 112, D03102.
Entekhabi, D., Njoku, E.G., O'Neill, P.E., Kellogg, K.H., Crow, W.T., Edelstein, W.N., Entin, J.K., Goodman, S.D., Jackson, T.J., Johnson, J., 2010a. The soil moisture active passive (SMAP) mission. Proc. IEEE 98, 704–716.
Entekhabi, D., Reichle, R.H., Koster, R.D., Crow, W.T., 2010b. Performance metrics for soil moisture retrievals and application requirements. J. Hydrometeorol. 11, 832–840.
Entekhabi, D., Yueh, S., O'Neill, P., Kellogg, K., Allen, A., Bindlish, R., Brown, M., Chan, S., Colliander, A., Crow, W., 2014. SMAP Handbook, JPL Publication JPL 400-1567, 182. Jet Propulsion Laboratory, Pasadena, California.
Fang, L., Hain, C.R., Zhan, X., Anderson, M.C., 2016. An inter-comparison of soil moisture data products from satellite remote sensing and a land surface model. Int. J. Appl. Earth Obs. Geoinf. 48, 37–50.
Figa-Saldaña, J., Wilson, J.J., Attema, E., Gelsthorpe, R., Drinkwater, M., Stoffelen, A., 2002. The advanced scatterometer (ASCAT) on the meteorological operational (MetOp) platform: a follow on for European wind scatterometers. Can. J. Remote Sens. 28, 404–412.
Gaiser, P.W., St Germain, K.M., Twarog, E.M., Poe, G.A., Purdy, W., Richardson, D., Grossman, W., Jones, W.L., Spencer, D., Golba, G., 2004. The WindSat spaceborne polarimetric microwave radiometer: sensor description and early orbit performance. IEEE Trans. Geosci. Remote Sens. 42, 2347–2361.
Gloersen, P., & Hardis, L. (1978). The scanning multichannel microwave radiometer (SMMR) experiment. In its The Nimbus 7 User's Guide p 213-246 (SEE N79-20148 11-12), 1, 213–246.
Gruber, A., Su, C.-H., Zwieback, S., Crow, W., Dorigo, W., Wagner, W., 2016. Recent advances in (soil moisture) triple collocation analysis. Int. J. Appl. Earth Observ. Geoinform. 45, 200–211.
Guillod, B.P., Orlowsky, B., Miralles, D.G., Teuling, A.J., Seneviratne, S.I., 2015. Reconciling spatial and temporal soil moisture effects on afternoon rainfall. Nat. Commun. 6 Article number 6443.
Jackson, T.J., 1997. Soil moisture estimation using special satellite microwave/imager satellite data over a grassland region. Water Resour. Res. 33, 1475–1484.
Jackson, T.J., Cosh, M.H., Bindlish, R., Starks, P.J., Bosch, D.D., Seyfried, M., Goodrich, D.C., Moran, M.S., Du, J., 2010. Validation of advanced microwave scanning radiometer soil moisture products. IEEE Trans. Geosci. Remote Sens. 48, 4256–4272.
Jackson, T.J., Hsu, A.Y., O'Neill, P.E., 2002. Surface soil moisture retrieval and mapping using high-frequency microwave satellite observations in the Southern Great Plains. J. Hydrometeorol. 3, 688–699.
Karthikeyan, L., Kumar, D.N., 2016. A novel approach to validate satellite soil moisture retrievals using precipitation data. J. Geophys. Res.: Atmosp. 121, 11516–11535. http://dx.doi.org/10.1002/2016JD024829.
Karthikeyan, L., Pan, M., Wanders, N., Kumar, D.N., Wood, E.F., 2017. Four decades of microwave satellite soil moisture observations: Part 1. A review of retrieval algorithms. Adv. Water Resour. http://dx.doi.org/10.1016/j.advwatres.2017.09.006.
Kawanishi, T., Sezai, T., Ito, Y., Imaoka, K., Takeshima, T., Ishido, Y., Shibata, A., Miura, M., Inahata, H., Spencer, R.W., 2003. The advanced microwave scanning radiometer for the earth observing system (AMSR-E), NASDA's contribution to the EOS for global energy and water cycle studies. IEEE Trans. Geosci. Remote Sens. 41, 184–194.
Kerr, Y.H., Al-Yaari, A., Rodriguez-Fernandez, N., Parrens, M., Molero, B., Leroux, D., Bircher, S., Mahmoodi, A., Mialon, A., Richaume, P., 2016. Overview of SMOS performance in terms of global soil moisture monitoring after six years in operation. Remote Sens. Environ. 180, 40–63.
Kerr, Y.H., Waldteufel, P., Richaume, P., Wigneron, J.P., Ferrazzoli, P., Mahmoodi, A., Al Bitar, A., Cabot, F., Gruhier, C., Juglea, S.E., 2012. The SMOS soil moisture retrieval algorithm. IEEE Trans. Geosci. Remote Sens. 50, 1384–1403.
Kerr, Y.H., Waldteufel, P., Wigneron, J.-P., Martinuzzi, J., Font, J., Berger, M., 2001. Soil moisture retrieval from space: the soil moisture and ocean salinity (SMOS) mission. IEEE Trans. Geosci. Remote Sens. 39, 1729–1735.
Koike, T., Nakamura, Y., Kaihotsu, I., Davaa, G., Matsuura, N., Tamagawa, K., Fujii, H., 2004. Development of an advanced microwave scanning radiometer (AMSR-E) algorithm for soil moisture and vegetation water content. Proc. Hydraul. Eng. 48, 217–222.
Koster, R.D., Dirmeyer, P.A., Guo, Z., Bonan, G., Chan, E., Cox, P., Gordon, C., Kanae, S., Kowalczyk, E., Lawrence, D., 2004. Regions of strong coupling between soil moisture and precipitation. Science 305, 1138–1140.
Koster, R.D., Guo, Z., Yang, R., Dirmeyer, P.A., Mitchell, K., Puma, M.J., 2009. On the nature of soil moisture in land surface models. J. Clim. 22, 4322–4335.
Liang, X., Lettenmaier, D.P., Wood, E.F., Burges, S.J., 1994. A simple hydrologically based model of land surface water and energy fluxes for general circulation models. J. Geophys. Res.: Atmos. 99, 14415–14428.
Liang, X., Wood, E.F., Lettenmaier, D.P., 1996. Surface soil moisture parameterization of the VIC-2L model: evaluation and modification. Global Planet Change 13, 195–206.
Liu, Y., Dorigo, W.A., Parinussa, R., de Jeu, R.A., Wagner, W., McCabe, M.F., Evans, J., Van Dijk, A., 2012. Trend-preserving blending of passive and active microwave soil moisture retrievals. Remote Sens. Environ. 123, 280–297.
Liu, Y.Y., Parinussa, R., Dorigo, W.A., De Jeu, R.A., Wagner, W., Van Dijk, A., McCabe, M.F., Evans, J., 2011. Developing an improved soil moisture dataset by blending passive and active microwave satellite-based retrievals. Hydrol. Earth Syst. Sci. 15, 425.
Luo, L., Wood, E.F., 2007. Monitoring and predicting the 2007 US drought. Geophys. Res. Lett. 34, L22702.
Maeda, T., Taniguchi, Y., 2013. Descriptions of GCOM-W1 AMSR2 Level 1R and Level 2 Algorithms. Japan Aerospace Exploration Agency Earth Observation Research Center. Ibaraki, Japan.
Massari, C., Brocca, L., Moramarco, T., Tramblay, Y., Lescot, J.-F.D., 2014. Potential of soil moisture observations in flood modelling: estimating initial conditions and correcting rainfall. Adv. Water Resour. 74, 44–53.
May, W., Meier, A., Rummukainen, M., Berg, A., Chéruy, F., Hagemann, S., 2015. Contributions of soil moisture interactions to climate change in the tropics in the GLACE–CMIP5 experiment. Clim. Dyn. 45, 3275–3297.
McCabe, M., Wood, E., Gao, H., 2005. Initial soil moisture retrievals from AMSRE: multiscale comparison using in situ data and rainfall patterns over Iowa. Geophys. Res. Lett. 32, L06403.
McColl, K.A., Alemohammad, S.H., Akbar, R., Konings, A.G., Yueh, S., Entekhabi, D., 2017. The global distribution and dynamics of surface soil moisture. Nat. Geosci 10, 100–104.
Miralles, D.G., Teuling, A.J., Van Heerwaarden, C.C., de Arellano, J.V.-G., 2014. Mega-heatwave temperatures due to combined soil desiccation and atmospheric heat accumulation. Nat. Geosci. 7, 345–349.
Mo, K.C., 2008. Model-based drought indices over the United States. J. Hydrometeorol. 9, 1212–1230.
Myneni, R., Hoffman, S., Knyazikhin, Y., Privette, J., Glassy, J., Tian, Y., Wang, Y., Song, X., Zhang, Y., Smith, G., 2002. Global products of vegetation leaf area and fraction absorbed PAR from year one of MODIS data. Remote Sens. Environ. 83, 214–231.
Njoku, E.G., Jackson, T.J., Lakshmi, V., Chan, T.K., Nghiem, S.V., 2003. Soil moisture retrieval from AMSR-E. IEEE Trans. Geosci. Remote Sens. 41, 215–229.
Njoku, E.G., Li, L., 1999. Retrieval of land surface parameters using passive microwave measurements at 6-18GHz. IEEE Trans. Geosci. Remote Sens. 37, 79–93.
Njoku, E.G., Rague, B., Fleming, K., 1998. Nimbus-7 SMMR Pathfinder Brightness Temperature Data Set. Jet Propulsion Laboratory, National Aeronautics and Space Administration.
Noll, J., Baptista, J.P., Buonomo, S., Rognes, A., 1994. Special sensor microwave/imager (SSM/I): instrument, data analysis and applications. In: Remote Sensing and Global Climate Change. Springer, pp. 119–133.
O'Neill, P., Chan, S., Njoku, E., Jackson, T., Bindlish, R., 2016a. Algorithm Theoretical Basis Document Level 2 & 3 Soil Moisture (Passive) Data Products. Jet Propulsion Laboratory, Pasadena, CA Revision C. SMAP Project, JPL D-66480.
O'Neill, P.E., Chan, S., Njoku, E.G., & Jackson, T.J. (2016b). SMAP L3 Radiometer Global Daily 36 km EASE-Grid Soil Moisture. Version 4. [R14010]. NASA National Snow and Ice Data Center Distributed Active Archive Center. (Ed.). Boulder, Colorado USA.
Orth, R., Seneviratne, S., 2013. Propagation of soil moisture memory to streamflow and evapotranspiration in Europe. Hydrol. Earth Syst. Sci. 17, 3895.
Owe, M., de Jeu, R., Holmes, T., 2008. Multisensor historical climatology of satellite derived global land surface moisture. J. Geophys. Res.: Earth Surf. 113, F01002.
Pan, M., Cai, X., Chaney, N.W., Entekhabi, D., Wood, E.F., 2016. An initial assessment of SMAP soil moisture retrievals using high resolution model simulations and in situ observations. Geophys. Res. Lett. 43, 9662–9668.
Pan, M., Fisher, C.K., Chaney, N.W., Zhan, W., Crow, W.T., Aires, F., Entekhabi, D., Wood, E.F., 2015. Triple collocation: beyond three estimates and separation of structural/non-structural errors. Remote Sens. Environ. 171, 299–310.
Pan, M., Sahoo, A.K., Wood, E.F., 2014. Improving soil moisture retrievals from a physically-based radiative transfer model. Remote Sens. Environ. 140, 130–140.
Pan, M., Wood, E.F., 2009. A multiscale ensemble filtering system for hydrologic data assimilation. Part II: application to land surface modeling with satellite rainfall forcing. J. Hydrometeorol. 10, 1493–1506.
Pan, M., Wood, E.F., 2010. Impact of accuracy, spatial availability, and revisit time of satellite-derived surface soil moisture in a multiscale ensemble data assimilation system. IEEE J. Select. Top. Appl. Earth Observat. Remote Sens. 3, 49–56.
Parinussa, R.M., Holmes, T.R., Wanders, N., Dorigo, W.A., de Jeu, R.A., 2015. A preliminary study toward consistent soil moisture from AMSR2. J. Hydrometeorol. 16, 932–947.
Parinussa, R.M., Lakshmi, V., Johnson, F.M., Sharma, A., 2016. A new framework for monitoring flood inundation using readily available satellite data. Geophys. Res. Lett 43, 2599–2605.
Peng, J., Niesel, J., Loew, A., Zhang, S., Wang, J., 2015. Evaluation of satellite and reanalysis soil moisture products over Southwest China using ground-based measurements. Remote Sens. 7, 15729–15747.
Piepmeier, J.R., Focardi, P., Horgan, K.A., Knuble, J., Ehsan, N., Lucey, J., Brambora, C., Brown, P.R., Hoffman, P.J., French, R.T., 2017. SMAP L-band microwave radiometer: instrument design and first year on orbit. IEEE Trans. Geosci. Remote Sens 55 (4), 1954–1966.
Prigent, C., Aires, F., Rossow, W.B., Robock, A., 2005. Sensitivity of satellite microwave and infrared observations to soil moisture at a global scale: relationship of satellite observations to in situ soil moisture measurements. J. Geophys. Res.: Atmosp. 110, D07110.
Reichle, R.H., Koster, R.D., 2004. Bias reduction in short records of satellite soil moisture. Geophys. Res. Lett. 31, L19501.
Reichle, R., Crow, W., Koster, R., Sharif, H., Mahanama, S., 2008. Contribution of soil moisture retrievals to land data assimilation products. Geophys. Res. Lett. 35, L01404.

Reichle, R.H., De Lannoy, G.J., Liu, Q., Ardizzone, J.V., Chen, F., Colliander, A., Conaty, A., Crow, W., Jackson, T., & Kimball, J. (2016). Soil Moisture Active Passive Mission L4_SM Data Product Assessment (Version 2 Validated Release).

Rosenzweig, C., Tubiello, F.N., Goldberg, R., Mills, E., Bloomfield, J., 2002. Increased crop damage in the US from excess precipitation under climate change. Global Environ. Change 12, 197–202.

Salvucci, G.D., 2001. Estimating the moisture dependence of root zone water loss using conditionally averaged precipitation. Water Resour. Res. 37, 1357–1365.

Scipal, K., Holmes, T., De Jeu, R., Naeimi, V., Wagner, W., 2008. A possible solution for the problem of estimating the error structure of global soil moisture data sets. Geophys. Res. Lett. 35, L24403.

Seneviratne, S.I., Corti, T., Davin, E.L., Hirschi, M., Jaeger, E.B., Lehner, I., Orlowsky, B., Teuling, A.J., 2010. Investigating soil moisture–climate interactions in a changing climate: a review. Earth-Sci. Rev. 99, 125–161.

Seneviratne, S.I., Wilhelm, M., Stanelle, T., Hurk, B., Hagemann, S., Berg, A., Cheruy, F., Higgins, M.E., Meier, A., Brovkin, V., 2013. Impact of soil moisture climate feedbacks on CMIP5 projections: first results from the GLACE CMIP5 experiment. Geophys. Res. Lett. 40, 5212–5217.

Sheffield, J., Wood, E.F., 2007. Characteristics of global and regional drought, 1950–2000: analysis of soil moisture data from offline simulation of the terrestrial hydrologic cycle. J. Geophys. Res.: Atmosp. 112, D17115.

Troy, T.J., Wood, E.F., Sheffield, J., 2008. An efficient calibration method for continental scale land surface modeling. Water Resour. Res. 44, W09411.

Tuttle, S.E., Salvucci, G.D., 2014. A new approach for validating satellite estimates of soil moisture using large-scale precipitation: comparing AMSR-E products. Remote Sens. Environ. 142, 207–222.

Ulaby, F., Moore, R., Fung, A., 1986. Microwave remote sensing: Active and passive. Volume 3-From theory to applications.

Vogel, M., Orth, R., Cheruy, F., Hagemann, S., Lorenz, R., Hurk, B., Seneviratne, S., 2017. Regional amplification of projected changes in extreme temperatures strongly controlled by soil moisture temperature feedbacks. Geophys. Res. Lett. 55, 1511–1519.

Wagner, W., Lemoine, G., Rott, H., 1999. A method for estimating soil moisture from ERS scatterometer and soil data. Remote Sens. Environ. 70, 191–207.

Wagner, W., Scipal, K., Pathe, C., Gerten, D., Lucht, W., Rudolf, B., 2003. Evaluation of the agreement between the first global remotely sensed soil moisture data with model and precipitation data. J. Geophys. Res.: Atmosp. 108.

Wanders, N., Bierkens, M.F., de Jong, S.M., de Roo, A., Karssenberg, D., 2014a. The benefits of using remotely sensed soil moisture in parameter identification of large scale hydrological models. Water Resour. Res. 50, 6874–6891.

Wanders, N., Karssenberg, D., Bierkens, M., Parinussa, R., de Jeu, R., van Dam, J., de Jong, S., 2012. Observation uncertainty of satellite soil moisture products determined with physically-based modeling. Remote Sens. Environ. 127, 341–356.

Wanders, N., Karssenberg, D., Roo, A.d., De Jong, S., Bierkens, M., 2014b. The suitability of remotely sensed soil moisture for improving operational flood forecasting. Hydrol. Earth Syst. Sci. 18, 2343–2357.

Wanders, N., Pan, M., Wood, E., 2015. Correction of real-time satellite precipitation with multi-sensor satellite observations of land surface variables. Remote Sens. Environ. 160, 206–221.

Wood, E., Pan, M., Sheffield, J., Vinukolu, R., Ferguson, C., Gao, H., Tang, Q., Shi, X., Zhu, C., Bohn, T., Su, F., Lettenmaier, D.P., Sahoo, A., De Lannoy, G., Houser, P., Pinker, R., Ma, Y., Li, C., Kummerow, C., 2009. Algorithm theoretical basis document for terrestrial water cycle data records. In: As part of National Aeronautic and Space Administration project Making Earth Science Data Records for Use in Research Environments, p. 244.

Wu, Q., Liu, H., Wang, L., Deng, C., 2016. Evaluation of AMSR2 soil moisture products over the contiguous United States using in situ data from the international soil moisture network. Int. J. Appl. Earth Observ. Geoinform. 45, 187–199.

Xia, Y., Ek, M., Wei, H., Meng, J., 2012. Comparative analysis of relationships between NLDAS2 forcings and model outputs. Hydrol. Process. 26, 467–474.

Yan, H., Moradkhani, H., 2016. Combined assimilation of streamflow and satellite soil moisture with the particle filter and geostatistical modeling. Adv. Water Resour. 94, 364–378.

Zhan, W., Pan, M., Wanders, N., Wood, E., 2015. Correction of real-time satellite precipitation with satellite soil moisture observations. Hydrol. Earth Syst. Sci. 19, 4275–4291.